FERMILAB-PUB-01/394-T
KEK-CP-119
YITP-01-90
hep-lat/0112045

Application of heavy-quark effective theory to lattice QCD: III. Radiative corrections to heavy-heavy currents

Junpei Harada,[1] Shoji Hashimoto,[2] Andreas S. Kronfeld,[3] and Tetsuya Onogi,[1,4*]
[1] *Department of Physics, Hiroshima University, Higashi-Hiroshima 739-8526, Japan*
[2] *High Energy Accelerator Research Organization (KEK), Tsukuba 305-0801, Japan*
[3] *Theoretical Physics Department, Fermi National Accelerator Laboratory, Batavia, Illinois 60510*
[4] *Yukawa Institute for Theoretical Physics, Kyoto University, Sakyo-ku, Kyoto 606-8502, Japan*
(21 December 2001)

Abstract

We apply heavy-quark effective theory (HQET) to separate long- and short-distance effects of heavy quarks in lattice gauge theory. In this paper we focus on flavor-changing currents that mediate transitions from one heavy flavor to another. We stress differences in the formalism for heavy-light currents, which are discussed in a companion paper, showing how HQET provides a systematic matching procedure. We obtain one-loop results for the matching factors of lattice currents, needed for heavy-quark phenomenology, such as the calculation of zero-recoil form factors for the semileptonic decays $B \to D^{(*)} l\nu$. Results for the Brodsky-Lepage-Mackenzie scale q^* are also given.

PACS numbers: 12.38.Gc, 13.20.He, 12.15.Hh

I. INTRODUCTION

This paper applies heavy-quark effective theory (HQET) to study the renormalization in lattice gauge theory of currents containing heavy quarks. It is a sequel to our papers on power corrections [1] and on radiative corrections to heavy-light currents [2]. Here we treat the case where one heavy quark flavor decays to another. To make contact with heavy-quark phenomenology, we denote the two flavors by the labels b and c. In the description of lattice gauge theory with HQET, discretization effects of the heavy quarks are absorbed into the short-distance coefficients of the effective Lagrangian and effective currents. The key difference between this work and Ref. [2] is that now, with two heavy flavors, HQET is used to describe both heavy quarks. Thus, the short-distance coefficients are functions of $m_b a$ and $m_c a$, where m_b and m_c are the heavy quark masses, and a is the lattice spacing.

Heavy-heavy currents are needed to calculate the zero-recoil form factors of the semileptonic decays $B \to Dl\nu$ and $B \to D^* l\nu$, as well as the change in the form factors away from zero recoil. These decays are of great phenomenological interest, because with reliable lattice calculations of $B \to D^{(*)}$ transitions one can make a model-independent determination of the element V_{cb} of the Cabibbo-Kobayashi-Maskawa (CKM) matrix. For further background on the impact of lattice matrix elements on CKM phenomenology see, for example, Refs. [3].

The application of HQET to lattice gauge theory began with the consideration of power corrections [1], building on the demonstration [4] that Wilson's formulation of lattice fermions [5] have a well-defined heavy quark limit. In particular, the Isgur-Wise heavy quark symmetries [6] emerge whenever the heavy-quark mass $m_h \gg \Lambda_{\rm QCD}$, even if $m_h \sim a^{-1}$. (The label h denotes a generic heavy flavor.) Because Wilson fermions have the the same symmetries and fields as continuum heavy quarks, on-shell lattice correlation functions can be described with HQET. This point of view is sometimes called the "non-relativistic interpretation" of lattice QCD [4].

In describing either lattice gauge theory or continuum QCD with HQET, physics at short distances is lumped into short-distance coefficients. Several short distances—two inverse heavy quark masses and (on the lattice) the lattice spacing—arise in the decay of one heavy flavor to another. The coefficients depend not only on $m_b a$ and $m_c a$, but also on other "irrelevant" parameters of the lattice action and currents. By adjusting these parameters of the action and currents, lattice gauge theory can be tuned, term by term, to the heavy-quark expansion of continuum QCD [4,1,2]. In this adjustment, details of HQET, such as its renormalization scheme, drop out. Matching with HQET is, thus, an intermediate conceptual step that explains how to match lattice gauge theory to QCD when $m_h a \not\ll 1$. It provides an attractive extension of more familiar matching procedures, such as those based on the Symanzik effective field theory [7–10], which usually assume $m_h a \ll 1$.

In addition to developing the formalism, which holds to all orders in perturbation theory, we compute the one-loop terms of the matching coefficients of the leading dimension vector and axial vector currents. We present compact expressions of the integrands of the momentum integration, for the Fermilab action and currents [4]. We also present numerical results for the Sheikholeslami-Wohlert (SW) [11] and Wilson [5] actions, which are the special cases most often used in the (non-relativistic interpretation of the) Fermilab heavy-quark method. We include the so-called rotation terms [12,4] in the currents, which are needed for tree-level matching at dimension four. It is also possible to obtain most of the normalization

non-perturbatively [13–15], and we give separately the residual short-distance correction.

Our perturbative results have been used in the calculation of the zero-recoil form factor for $B \to D^* l\nu$ [14] and, indirectly, in the calculation for form factors for $B \to \pi l\nu$ [15]. One-loop results without the rotation were given in a preliminary report of this work [16], and used in the calculation of the zero-recoil form factors for $B \to Dl\nu$ [13].

This paper is organized along the lines Ref. [2]. Section II discusses how to use HQET to separate long- and short-distance physics with (continuum) effective field theories. In particular, we obtain a definition of the matching factors of the heavy-heavy vector and axial vector currents. Section III introduces a specific definition of lattice currents suited to improvement in the HQET matching procedure; these currents generalize those used recently for $B \to D^{(*)}$ matrix elements [13,14]. In Sec. IV we present one-loop results for the matching factors, including the scale q^* in the Brodsky-Lepage-Mackenzie (BLM) scale-setting prescription [17,18]. Some concluding remarks are made in Sec. V. Three appendices contain details of the one-loop calculation, including an outline of a method to obtain compact expressions, and explicit results for the one-loop Feynman integrands for the vertex functions with the Fermilab action.

Instead of printing tables of the numerical results in Sec. IV, we are making a suite of programs freely available [19]. This suite includes programs for the heavy-light currents treated in our companion paper [2].

II. MATCHING WITH HQET

In our companion paper [2] we reviewed how the standard Symanzik description of cutoff effects breaks down when $m_h a \not\ll 1$. It is worth re-emphasizing that it is the *description* that breaks down—particularly the Taylor series of short-distance coefficients in powers of $m_h a$. Lattice gauge theory remains well-defined for all $m_h a$, but one needs other tools to understand how to relate lattice observables to continuum QCD. The obvious alternatives are the effective field theories HQET [20–24] and NRQCD [25,26], which exploit the simpler dynamics of systems with one or more heavy quarks. The simpler dynamics also emerge in lattice gauge theory with massive fermions, so the effective theories also can be re-applied to understand lattice observables [1,2,4].

In this section we show, in the case of heavy-heavy currents, how to use HQET to match lattice gauge theory to continuum QCD. We first recall the HQET description of heavy-heavy currents in continuum QCD, paralleling the discussion in Ref. [2]. We then explain what changes are needed to describe lattice gauge theory with heavy fermions. We focus on HQET because of the phenomenological importance of $B \to D^{(*)}$ transitions; for quarkonium the logic could be repeated with NRQCD velocity-counting rules [25,26]. Unlike the standard Symanzik program [7–10], the HQET approach works even in the region where $m_h a$ is no longer small. Like the usual HQET, however, it requires ($\boldsymbol{p}$ is a typical momentum)

$$m_h \gg \boldsymbol{p},\, \Lambda_{\rm QCD}, \tag{2.1}$$

but once this condition holds (and $\boldsymbol{p}a \ll 1$), our formalism provides a systematic description of lattice observables for all $m_h a$, $h = b,\, c$.

The conventions for HQET are the same as those given Sec. III of Ref. [1]. Each HQET quark field carries a velocity label. For the time being we use two different velocities, v and v', for the two flavors. The velocities can be chosen somewhat arbitrarily, but HQET is a good description of QCD if each is close to the velocity of the hadron containing the heavy quark.[1] The fourth Euclidean component $v_4 = iv^0$, so in the rest frame $v = (i, \mathbf{0})$, and similarly for v'. The metric is taken to be $\mathrm{diag}(\pm 1, 1, 1, 1)$, with the upper (lower) sign for Euclidean (Minkowski) spacetime. In either case, $v^2 = v'^2 = -1$. We denote the two HQET fields as $\bar{c}_{v'}$ and b_v. When the flavor of quark is unimportant, we write formulas with the more generic symbol h_v. The HQET field h_v satisfies the constraint $\frac{1}{2}(1 - i\not{v})h_v = h_v$, or

$$\not{v} b_v = i b_v, \quad \bar{c}_{v'} \not{v}' = i \bar{c}_{v'}. \tag{2.2}$$

Physically this constraint means that only quarks, but not anti-quarks, are described. The tensor $\eta^\mu_\nu = \delta^\mu_\nu + v^\mu v_\nu$ projects onto components orthogonal to v. For a vector p, the component orthogonal to v is $p^\mu_\perp = \eta^\mu_\nu p^\nu = p^\mu + v^\mu v \cdot p$. In the rest frame, these are the spatial components. Similarly, $\eta'^\mu_\nu = \delta^\mu_\nu + v'^\mu v'_\nu$, and $p^\mu_{\perp'} = \eta'^\mu_\nu p^\nu$.

HQET describes the dynamics of heavy-light bound states with an effective Lagrangian built from $c_{v'}$ and b_v. For each flavor one writes

$$\mathcal{L}_{\mathrm{QCD}} = -\bar{q}(\not{D} + m)q \doteq \mathcal{L}_{\mathrm{HQET}}, \tag{2.3}$$

where the symbol $\doteq$ means "has the same on-shell matrix elements as". The HQET Lagrangian consists of a series of sets of terms

$$\mathcal{L}_{\mathrm{HQET}} = \mathcal{L}^{(0)} + \mathcal{L}^{(1)} + \mathcal{L}^{(2)} + \cdots, \tag{2.4}$$

where $\mathcal{L}^{(s)}$ consists of all operators of dimension $s + 4$ built out of $\bar{h}_v$ and h_v (and gluons and light quarks). The ultraviolet regulator and renormalization scheme of the two sides of Eq. (2.3) need not be the same. For the aims of this paper it is enough to consider the first two terms, $\mathcal{L}^{(0)}$ and $\mathcal{L}^{(1)}$, but the generalization to higher dimension should be clear.

The leading, dimension-four term is

$$\mathcal{L}^{(0)} = \bar{h}_v(iv \cdot D - m_h)h_v, \tag{2.5}$$

where m_h is the mass of flavor h. $\mathcal{L}^{(0)}$ is a good starting point for the heavy-quark expansion, which treats the higher-dimension operators as small. The mass term in $\mathcal{L}^{(0)}$ is usually omitted, because it obscures the heavy-quark flavor symmetry (though only slightly [1]). By heavy-quark symmetry, it has an effect neither on bound-state wave functions nor, consequently, on matrix elements. It does affect the mass spectrum, but only additively.

When the mass term is included, higher-dimension operators are constructed with $\mathcal{D}^\mu = D^\mu - iMv^\mu$ and $\mathcal{D}' = D^\mu - iMv'$. Here M selects the mass of flavor h: $Mh_v = m_h h_v$.

---

[1] In NRQCD, the relative velocity between the heavy quark and heavy anti-quark of quarkonium should not be confused with the velocities v and v' introduced here. Note that it is also possible to formulate NRQCD with a total velocity label like v [27,28].

To describe on-shell matrix elements one may omit operators that vanish by the equations of motion, $-iv\cdot\mathcal{D}b_v = 0$ and $\bar{c}_{v'} iv'\cdot\overleftarrow{\mathcal{D}}' = 0$, In practice, higher dimension operators are constructed with $\mathcal{D}^\mu_\perp = D^\mu_\perp$ (or, for velocity v', $D^\mu_{\perp'}$) and $[\mathcal{D}^\mu, \mathcal{D}^\nu] = [D^\mu, D^\nu] = F^{\mu\nu}$. The dimension-five terms in the Lagrangian are

$$\mathcal{L}^{(1)} = \mathcal{C}_2\mathcal{O}_2 + \mathcal{C}_\mathcal{B}\mathcal{O}_\mathcal{B}, \tag{2.6}$$

where $\mathcal{C}_2$ and $\mathcal{C}_\mathcal{B}$ are short-distance coefficients, and

$$\mathcal{O}_2 = \bar{h}_v D^2_\perp h_v, \tag{2.7}$$
$$\mathcal{O}_\mathcal{B} = \bar{h}_v s_{\alpha\beta} B^{\alpha\beta} h_v, \tag{2.8}$$

with $s_{\alpha\beta} = -i\sigma_{\alpha\beta}/2$ and $B^{\alpha\beta} = \eta^\alpha_\mu \eta^\beta_\nu F^{\mu\nu}$. In operators with two HQET fields (for flavor-changing currents, say) $\overleftarrow{\mathcal{D}}'$ and $\mathcal{D}$ appear together.

In Eq. (2.5) one should think of the quark mass m_h as a short-distance coefficient. By reparametrization invariance [29] and Lorentz invariance of (continuum) QCD, the same mass appears in the short-distance coefficient of the kinetic energy $\mathcal{C}_2\mathcal{O}_2$, namely,

$$\mathcal{C}_2 = \frac{1}{2m_h}. \tag{2.9}$$

If the operators of HQET are renormalized with a minimal subtraction in dimensional regularization, then m_h is the (perturbative) pole mass. The chromomagnetic operator $\mathcal{O}_\mathcal{B}$ depends on the renormalization point μ of HQET, and that dependence is canceled by

$$\mathcal{C}_\mathcal{B}(\mu) = \frac{z_\mathcal{B}(\mu)}{2m_h}. \tag{2.10}$$

The description of flavor-changing currents proceeds along similar lines. Let

$$\mathcal{V}^\mu = \bar{c} i\gamma^\mu b \tag{2.11}$$

be the flavor-changing vector current, where $\bar{c}$ and b without the velocity subscripts are QCD fields obeying the Dirac equation. In HQET $\mathcal{V}^\mu$ is described by

$$\mathcal{V}^\mu \doteq \bar{C}_{V_\parallel} v^\mu \bar{c}_{v'} b_v + \bar{C}_{V_\perp} \bar{c}_{v'} i\gamma^\mu_\perp b_v + \bar{C}_{V_{v'}} v'^\mu_\perp \bar{c}_{v'} b_v - \sum_{i=1}^{14} \bar{B}_{Vi} \bar{\mathcal{Q}}^\mu_{Vi} + \cdots, \tag{2.12}$$

where $\bar{c}_{v'}$ and b_v are HQET fields, which satisfy Eq. (2.4) and whose dynamics are given by $\mathcal{L}_{\rm HQET}$. The fourteen dimension-four operators are

$$\bar{\mathcal{Q}}^\mu_{V1} = -v^\mu \bar{c}_{v'} \not{D}_\perp b_v, \tag{2.13}$$
$$\bar{\mathcal{Q}}^\mu_{V2} = \bar{c}_{v'} i\gamma^\mu_\perp \not{D}_\perp b_v, \tag{2.14}$$
$$\bar{\mathcal{Q}}^\mu_{V3} = \bar{c}_{v'} i D^\mu_\perp b_v, \tag{2.15}$$
$$\bar{\mathcal{Q}}^\mu_{V4} = +v^\mu \bar{c}_{v'} \overleftarrow{\not{D}}_{\perp'} b_v, \tag{2.16}$$
$$\bar{\mathcal{Q}}^\mu_{V5} = \bar{c}_{v'} \overleftarrow{\not{D}}_{\perp'} i\gamma^\mu_{\perp'} b_v, \tag{2.17}$$

$$\bar{\mathcal{Q}}^\mu_{V6} = \bar{c}_{v'} i \overleftarrow{D}^\mu_{\perp'} b_v, \tag{2.18}$$
$$\bar{\mathcal{Q}}^\mu_{V7} = -v'^\mu_\perp \bar{c}_{v'} \not{D}_\perp b_v, \tag{2.19}$$
$$\bar{\mathcal{Q}}^\mu_{V8} = -v'^\mu_\perp \bar{c}_{v'} \overleftarrow{\not{D}}_{\perp'} b_v, \tag{2.20}$$
$$\bar{\mathcal{Q}}^\mu_{V9} = -v^\mu \bar{c}_{v'} iv' \cdot D_\perp b_v, \tag{2.21}$$
$$\bar{\mathcal{Q}}^\mu_{V10} = \bar{c}_{v'} i\gamma^\mu_\perp iv' \cdot D_\perp b_v, \tag{2.22}$$
$$\bar{\mathcal{Q}}^\mu_{V11} = -v^\mu \bar{c}_{v'} iv \cdot \overleftarrow{D}_{\perp'} b_v, \tag{2.23}$$
$$\bar{\mathcal{Q}}^\mu_{V12} = \bar{c}_{v'} iv \cdot \overleftarrow{D}_{\perp'} i\gamma^\mu_{\perp'} b_v, \tag{2.24}$$
$$\bar{\mathcal{Q}}^\mu_{V13} = -v'^\mu_\perp \bar{c}_{v'} iv' \cdot D_\perp b_v, \tag{2.25}$$
$$\bar{\mathcal{Q}}^\mu_{V14} = -v'^\mu_\perp \bar{c}_{v'} iv \cdot \overleftarrow{D}_{\perp'} b_v. \tag{2.26}$$

Further dimension-four operators are omitted, because they are linear combinations of those listed and others that vanish by the equations of motion. In developing the heavy-quark expansion the appropriate equations of motion for the heavy quarks are $(-iv\cdot\mathcal{D})b_v = 0$ and $\bar{c}_{v'}(iv'\cdot\overleftarrow{\mathcal{D}}') = 0$, derived from the respective $\mathcal{L}^{(0)}$.

The QCD axial vector current is

$$\mathcal{A}^\mu = \bar{c} i\gamma^\mu\gamma_5 b, \tag{2.27}$$

where $\bar{c}$ and b are again Dirac fields. $\mathcal{A}$ has an HQET description analogous to Eq. (2.12),

$$\mathcal{A}^\mu \doteq \bar{C}_{A_\perp} \bar{c}_{v'} i\gamma^\mu_\perp \gamma_5 b_v - \bar{C}_{A_\parallel} v^\mu \bar{c}_{v'}\gamma_5 b_v - \bar{C}_{A_{v'}} v'^\mu_\perp \bar{c}_{v'}\gamma_5 b_v - \sum_{i=1}^{14} \bar{B}_{Ai} \bar{\mathcal{Q}}^\mu_{Ai} + \cdots. \tag{2.28}$$

By convention, each operator $\bar{\mathcal{Q}}^\mu_{Ai}$ is obtained from $\bar{\mathcal{Q}}^\mu_{Vi}$ by replacing $\bar{c}_{v'}$ with $-\bar{c}_{v'}\gamma_5$.

The coefficients $\bar{C}_J$ and $\bar{B}_{Ji}$ and the operators $\bar{\mathcal{Q}}_{Ji}$ play an analogous role to the coefficients C_J and B_{Ji} and the operators $\mathcal{Q}_{Ji}$ introduced in Ref. [2], but they are not the same. The latter are defined in an effective theory using a Dirac field $\bar{q}$ (without a velocity label) to describe the light(er) quark, whereas the barred symbols are defined in a theory using an HQET field $\bar{c}_{v'}$ (with a velocity label) to describe the lighter (heavy) quark. The bars are used here to emphasize the difference.

There are many fewer operators when $v' = v$. One set of operators vanishes because $v'_\perp \to v_\perp = 0$, namely, $\bar{\mathcal{Q}}^\mu_{J7}$, $\bar{\mathcal{Q}}^\mu_{J8}$, $\bar{\mathcal{Q}}^\mu_{J13}$. $\bar{\mathcal{Q}}^\mu_{J14}$; another set vanishes because $v'\cdot D_\perp$, $v\cdot D_{\perp'} \to v\cdot D_\perp = 0$, namely, $\bar{\mathcal{Q}}^\mu_{Jj}$, $j \ge 9$. A last set vanishes because $P_+(v)\Gamma P_+(v) = 0$, where Γ stands for the full Dirac structure sandwiched by $\bar{c}_v$ and b_v. In the end, one is left with only $v^\mu \bar{c}_v b_v$, $\bar{\mathcal{Q}}^\mu_{V2}$, $\bar{\mathcal{Q}}^\mu_{V3}$, $\bar{\mathcal{Q}}^\mu_{V5}$, and $\bar{\mathcal{Q}}^\mu_{V6}$ for the vector current, and $\bar{c}_v i\gamma^\mu_\perp\gamma_5 b_v$, $\bar{\mathcal{Q}}^\mu_{A1}$, and $\bar{\mathcal{Q}}^\mu_{A4}$ for the axial vector current.

The coefficients of the HQET operators depend on the heavy-quark masses m_b and m_c (to balance dimensions), as well as m_c/m_b and μ/m_b, where μ is the renormalization scale. At the two-loop level and beyond, dependence on light quark masses m_q also appears. With two velocities, the coefficients also depend on $w = -v'\cdot v$. Although they are not needed below, it is instructive to give the coefficients of the dimension-three terms. At the tree level $\bar{C}^{[0]}_{J_\parallel} = \bar{C}^{[0]}_{J_\perp} = 1$ and $\bar{C}^{[0]}_{J_{v'}} = 0$. Through one loop order, for $v' = v$,

$$\bar{C}_{V_\parallel} = 1 + C_F \frac{g^2(\mu)}{16\pi^2} 3 f(m_c/m_b), \tag{2.29}$$

$$\bar{C}_{A_\perp} = 1 + C_F \frac{g^2(\mu)}{16\pi^2} \left[3 f(m_c/m_b) - 2\right], \tag{2.30}$$

where

$$f(z) = \frac{z+1}{z-1} \ln z - 2. \tag{2.31}$$

The important properties of $f(z)$ are $f(1) = 0$, $f(1/z) = f(z)$. At this order, μ dependence appears only in the renormalized coupling $g^2(\mu)$. The "non-f" part of $\bar{C}_{A_\perp}$ given here assumes that the renormalized axial current satisfies the axial Ward identity [30]. At the tree level, the coefficients of the dimension-four currents are

$$\bar{B}^{[0]}_{V1} = \bar{B}^{[0]}_{V2} = \frac{1}{2m_b} = +\bar{B}^{[0]}_{A1} = +\bar{B}^{[0]}_{A2} \tag{2.32}$$

$$\bar{B}^{[0]}_{V4} = \bar{B}^{[0]}_{V5} = \frac{1}{2m_c} = -\bar{B}^{[0]}_{A4} = -\bar{B}^{[0]}_{A5} \tag{2.33}$$

$$\bar{B}^{[0]}_{Ji} = 0, \quad \text{otherwise}, \tag{2.34}$$

but all become non-trivial when radiative corrections are included.

HQET provides a systematic way to separate the short distances $1/m_c$ and $1/m_b$ from the long distance $\Lambda_{\rm QCD}$, as long as the condition (2.1) holds for both flavors. HQET can also be applied to lattice gauge theory with the same structure and logic, treating a as another short distance. The strategy is viable as long as condition (2.1) holds and, of course, $\boldsymbol{p}a \ll 1$. For lattice NRQCD applied to heavy-light systems, HQET is just the corresponding Symanzik effective field theory. HQET may also be applied to Wilson fermions, because they have the correct particle content and heavy-quark symmetries as QCD [1]. Thus, for a lattice gauge theory with either NRQCD or Wilson quarks

$$\mathcal{L}_{\rm lat} \doteq \mathcal{L}_{\rm HQET}. \tag{2.35}$$

The effective Lagrangian $\mathcal{L}_{\rm HQET}$ has the same long-distance operators as in Eq. (2.3). The lattice modifies the short-distance behavior, so lattice artifacts of the heavy quarks should be lumped into the HQET coefficients [1]. For example, in the dimension-four HQET Lagrangian $\mathcal{L}^{(0)}$, one must replace m_h with the lattice rest mass m_{1h}.

Starting with $\mathcal{L}^{(3)}$ one must introduce operators to describe lattice violations of rotational invariance. An example is the dimension-seven operator $\mathcal{O}_4 = \sum_\mu \bar{h}_v (D^\mu_\perp)^4 h_v$. Such operators do not, of course, appear in the HQET description of continuum QCD, but they do not upset the general framework. They can still be defined as insertions in a continuum-regulated theory (analogously to operators like $\sum_\mu \bar{q}(D^\mu)^4 q$ in a Symanzik effective field theory). Because the symmetry-breaking arises at short-distances, it is more useful to focus on the operators' coefficients, noting that $\mathcal{C}_4^{\rm lat} \neq 0$, instead of $\mathcal{C}_4 = 0$ as for continuum QCD.

Returning to $\mathcal{L}^{(0)}$ and $\mathcal{L}^{(1)}$, the coefficient of the kinetic energy becomes

$$\mathcal{C}_2^{\rm lat} = \frac{1}{2m_{2h}}, \tag{2.36}$$

and m_{2h} is called the kinetic mass. If the HQET operators are defined by minimal subtraction in dimensional regularization, then both m_{1h} and m_{2h} can be computed from the pole in the perturbative quark propagator [33], and they are infrared finite and gauge independent [34]. The lattice breaks Lorentz (or Euclidean) invariance, so reparametrization invariance no longer requires m_{2h} to equal m_{1h}.

For the flavor-changing currents, one forms bilinears of lattice fermions fields with the right quantum numbers. Any such lattice currents for $b \to c$ can be described by

$$V^\mu_{\rm lat} \doteq \bar C^{\rm lat}_{V_\parallel} v^\mu \bar c_{v'} b_v + \bar C^{\rm lat}_{V_\perp} \bar c_{v'} i\gamma^\mu_\perp b_v + \bar C^{\rm lat}_{V_{v'}} v'^\mu_\perp \bar c_{v'} b_v - \sum_{i=1}^{14} \bar B^{\rm lat}_{Vi} \bar{\mathcal{Q}}^\mu_{Vi} + \cdots, \tag{2.37}$$

$$A^\mu_{\rm lat} \doteq \bar C^{\rm lat}_{A_\perp} \bar c_{v'} i\gamma^\mu_\perp \gamma_5 b_v - \bar C^{\rm lat}_{A_\parallel} v^\mu \bar c_{v'} \gamma_5 b_v - \bar C^{\rm lat}_{A_{v'}} v'^\mu_\perp \bar c_{v'} \gamma_5 b_v - \sum_{i=1}^{14} \bar B^{\rm lat}_{Ai} \bar{\mathcal{Q}}^\mu_{Ai} + \cdots. \tag{2.38}$$

An explicit construction of $V^\mu_{\rm lat}$ and $A^\mu_{\rm lat}$ through dimension 4 is given for Wilson fermions in Sec. III, and for lattice NRQCD already in Ref. [32]. On the right-hand side the HQET operators $\bar{\mathcal{Q}}_{Ji}$ are the same as in Eqs. (2.12) and (2.28), but the short-distance coefficients $\bar C^{\rm lat}_{J_{\parallel,\perp,v'}}$ and $\bar B^{\rm lat}_{Ji}$ are modified. In particular, they depend on the lattice spacing a through $m_b a$ or $m_c a$, and also on adjustable improvement parameters in $V^\mu_{\rm lat}$ and $A^\mu_{\rm lat}$. At and beyond the dimension six, there are HQET operators to describe violations of rotational invariance in the lattice currents, but, as above, they do not spoil the overall framework.

Since Eqs. (2.13)–(2.26) give a complete set of dimension-four HQET currents, the coefficients $\bar C^{\rm lat}_{J_\parallel, J_\perp}$ and $\bar B^{\rm lat}_{Ji}$ contain short-distance effects from both heavy quarks. For HQET operators of dimension $s+3$, the corresponding coefficient must contain s powers of the short distances m_b^{-1}, m_c^{-1} or a. Since they are functions of all ratios of short distances, it is a matter of choice which dimensionful quantity is factored out. The key point is that, even when applied to lattice gauge theory, the heavy-quark expansion is still a successive approximation: higher terms in the expansion are suppressed by powers of $\Lambda_{\rm QCD}$, with the dimensions balanced by the short distances.

Lattice artifacts from gluons and light quarks can be described by the Symanzik formalism [7–10]. At some level the light quarks will influence the HQET coefficients of the heavy quarks, and the heavy quarks will influence the Symanzik coefficients of the gluons and light quarks. These are, however, details that do not obstruct the central idea of using effective field theories to separate long- and short-distance physics.

The abstract ideas can be made more concrete by comparing the HQET descriptions of continuum and lattice matrix elements. The continuum matrix element of $v\cdot\mathcal{V}$ is

$$\begin{aligned}
\langle D|v\cdot\mathcal{V}|B\rangle = {} & -\bar C_{V_\parallel} \langle D^{(0)}_{v'}|\bar c_{v'} b_v|B^{(0)}_v\rangle - \sum_{i\in S_\parallel} \bar B_{Vi} \langle D^{(0)}_{v'}|v\cdot\bar{\mathcal{Q}}_{Vi}|B^{(0)}_v\rangle \\
& - \mathcal{C}_{2c}\bar C_{V_\parallel} \int d^4x \langle D^{(0)}_{v'}|T\,\mathcal{O}_{2c}(x)\bar c_{v'} b_v|B^{(0)}_v\rangle^\star \\
& - \mathcal{C}_{\mathcal{B}c}\bar C_{V_\parallel} \int d^4x \langle D^{(0)}_{v'}|T\,\mathcal{O}_{\mathcal{B}c}(x)\bar c_{v'} b_v|B^{(0)}_v\rangle^\star \\
& - \mathcal{C}_{2b}\bar C_{V_\parallel} \int d^4x \langle D^{(0)}_{v'}|T\,\bar c_{v'} b_v \mathcal{O}_{2b}(x)|B^{(0)}_v\rangle^\star \\
& - \mathcal{C}_{\mathcal{B}b}\bar C_{V_\parallel} \int d^4x \langle D^{(0)}_{v'}|T\,\bar c_{v'} b_v \mathcal{O}_{\mathcal{B}b}(x)|B^{(0)}_v\rangle^\star + O(\Lambda^2/m^2),
\end{aligned} \tag{2.39}$$

where the set $S_\parallel = \{1, 4, 9, 11\}$, and B (D) is any b-flavored (charmed) hadronic state. (The $\star$-ed T product is defined in Ref. [1]; this detail is unimportant here.) On the left-hand side the states are QCD eigenstates; on the right-hand side (with velocity subscripts) they are the corresponding eigenstates of $\mathcal{L}^{(0)}$, the leading HQET Lagrangian. The extra subscripts on the coefficients and operators from $\mathcal{L}^{(1)}$ denote flavor. The corresponding lattice matrix element is similar, but slightly different:

$$\begin{aligned}
\langle D|v\cdot V_{\rm lat}|B\rangle = &-\bar{C}^{\rm lat}_{V_\parallel}\langle D^{(0)}_{v'}|\bar{c}_{v'}b_v|B^{(0)}_v\rangle - \sum_{i\in S_\parallel}\bar{B}^{\rm lat}_{Vi}\langle D^{(0)}_{v'}|v\cdot\bar{\mathcal{Q}}_{Vi}|B^{(0)}_v\rangle \\
&- \mathcal{C}^{\rm lat}_{2c}\bar{C}^{\rm lat}_{V_\parallel}\int d^4x\langle D^{(0)}_{v'}|T\,\mathcal{O}_{2c}(x)\bar{c}_{v'}b_v|B^{(0)}_v\rangle^\star \\
&- \mathcal{C}^{\rm lat}_{\mathcal{B}c}\bar{C}^{\rm lat}_{V_\parallel}\int d^4x\langle D^{(0)}_{v'}|T\,\mathcal{O}_{\mathcal{B}c}(x)\bar{c}_{v'}b_v|B^{(0)}_v\rangle^\star \\
&- \mathcal{C}^{\rm lat}_{2b}\bar{C}^{\rm lat}_{V_\parallel}\int d^4x\langle D^{(0)}_{v'}|T\,\bar{c}_{v'}b_v\mathcal{O}_{2b}(x)|B^{(0)}_v\rangle^\star \\
&- \mathcal{C}^{\rm lat}_{\mathcal{B}b}\bar{C}^{\rm lat}_{V_\parallel}\int d^4x\langle D^{(0)}_{v'}|T\,\bar{c}_{v'}b_v\mathcal{O}_{\mathcal{B}b}(x)|B^{(0)}_v\rangle^\star \\
&+ K_{\sigma\cdot F}C^{\rm lat}_{V_\parallel}\int d^4x\langle D^{(0)}_{v'}|T\,\bar{c}_{v'}b_v\bar{q}i\sigma Fq(x)|B^{(0)}_v\rangle^\star + O(\Lambda^2a^2b(ma)).
\end{aligned} \tag{2.40}$$

Now the states on the left-hand side are lattice eigenstates. But on the right-hand side the differences compared to Eq. (2.39) are all in the coefficients: except for the last matrix element, they are, term by term, the same. The last T-product arise from the Symanzik local effective Lagrangian for light quarks, cf. Ref. [2].

Similar formulas hold for matrix elements of $\mathcal{V}^\mu_\perp$ and $V^\mu_{{\rm lat}\perp}$, and for the axial vector current. If one multiplies the lattice matrix elements with

$$\bar{Z}_{J_\parallel} = \frac{\bar{C}_{J_\parallel}}{\bar{C}^{\rm lat}_{J_\parallel}}, \tag{2.41}$$

$$\bar{Z}_{J_\perp} = \frac{\bar{C}_{J_\perp}}{\bar{C}^{\rm lat}_{J_\perp}}, \tag{2.42}$$

and subtracts the lattice from the continuum equations, a simple picture of cutoff effects emerges: lattice artifacts of the heavy quark are isolated into the mismatch of the short-distance coefficients, namely,

$$\delta\mathcal{C}_i = \mathcal{C}^{\rm lat}_i - \mathcal{C}_i, \tag{2.43}$$

$$\delta\bar{B}_{Ji} = \bar{Z}_{Ji}\bar{B}^{\rm lat}_{Ji} - \bar{B}_{Ji}. \tag{2.44}$$

In the lattice term of $\delta\bar{B}_{Ji}$, matching factors $\bar{Z}_{Ji}$ appear to restore a canonical normalization to the lattice currents. One has $\bar{Z}_{Ji} = \bar{Z}_{J_\parallel}$ for $i \in S_\parallel$, and $\bar{Z}_{Ji} = \bar{Z}_{J_\perp}$ for $i \in S_\perp = \{2, 3, 5, 6, 7, 8, 10, 12, 13, 14\}$.

The matching factors $\bar{Z}_{J_\parallel}$ and $\bar{Z}_{J_\perp}$ play the following role, sketched in Fig. 1. The denominator converts a lattice-regulated scheme to a renormalized HQET scheme, and the numerator converts the latter to a renormalized (continuum) QCD scheme. As long as the same HQET scheme is used, HQET drops out of the calculation of $\bar{Z}_{J_\parallel}$ and $\bar{Z}_{J_\perp}$. Moreover, changes in continuum renormalization conventions modify only the numerator, and changes

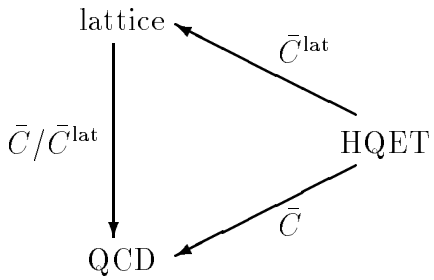

FIG. 1. Diagram illustrating how the matching factors $\bar{C}^{\rm lat}$, $\bar{C}$, and $\bar{Z} = \bar{C}/\bar{C}^{\rm lat}$ match lattice gauge theory and QCD to HQET, and to each other.

in the lattice action or currents modify only the denominator. Thus, the matching factors $\bar{Z}_{J_\parallel}$ and $\bar{Z}_{J_\perp}$ play the same role as the factors $Z_{J_\parallel}$ and $Z_{J_\perp}$ in HQET matching for heavy-light currents [2].

When HQET matching is applied to Wilson quarks, it is possible that the lighter heavy quark satisfies $m_c a \ll 1$. Then one could equally well apply the heavy-"light" formalism of Ref. [2], describing the charmed quark à la Symanzik with a Dirac field. This regime is interesting because in practice one often has $m_c a < \frac{1}{3}$ and $\Lambda/2m_c a < \frac{1}{3}$, so both the Symanzik and the HQET descriptions are reasonably accurate.

By comparing the two matching procedures, one can derive relations between the two sets of short-distance coefficients.[2] To proceed, one must introduce coefficients to relate the heavy-"light" theory with the Dirac field $\bar{c}$ to the heavy-"heavy" theory with the HQET field $\bar{c}_{v'}$:

$$\bar{c} b_v \doteq \breve{C}_{V_\parallel} \bar{c}_{v'} b_v + \sum_{i \in S_\parallel} \breve{B}_{Vi}\, v \cdot \bar{\mathcal{Q}}_{Vi} + \cdots, \tag{2.45}$$

$$\bar{c} i\gamma_\perp^\mu b_v \doteq \breve{C}_{V_\perp} \bar{c}_{v'} i\gamma_\perp^\mu b_v + \breve{C}_{V_{v'}} v'^\mu_\perp \bar{c}_{v'} b_v - \sum_{i \in S_\perp} \breve{B}_{Vi}\, \eta_\nu^\mu \bar{\mathcal{Q}}^\nu_{Vi} + \cdots, \tag{2.46}$$

$$\mathcal{Q}_{Vi} \doteq \sum_{j=1}^{14} \breve{C}_{Vij} \bar{\mathcal{Q}}_{Vj} + \cdots, \quad i = 1, 6, \tag{2.47}$$

and similarly for the axial vector current. The relation between the three sets of short-distance coefficients—$\bar{C}$ and $\bar{B}$, C and B, and $\breve{C}$ and $\breve{B}$—is sketched in Fig. 2. By substituting Eqs. (2.45)–(2.47) into Eq. (2.40) of Ref. [2] and comparing to the above Eq. (2.37), one finds (when $m_c a \ll 1$)

$$\bar{C}^{\rm lat}_{J_\parallel} = C^{\rm lat}_{J_\parallel} \breve{C}_{J_\parallel} \tag{2.48}$$

$$\bar{C}^{\rm lat}_{J_\perp} = C^{\rm lat}_{J_\perp} \breve{C}_{J_\perp} \tag{2.49}$$

$$\bar{C}^{\rm lat}_{J_{v'}} = C^{\rm lat}_{J_\perp} \breve{C}_{J_{v'}} \tag{2.50}$$

---

[2]One must take the same lattice currents. The improved currents of Ref. [2] and Sec. III are nearly the same.

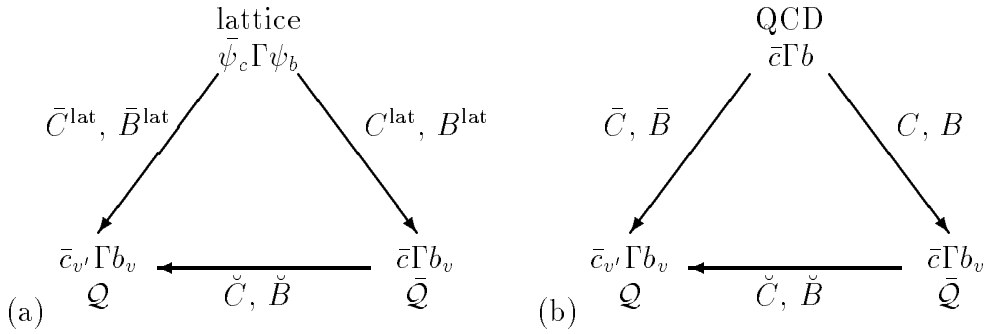

FIG. 2. Diagrams illustrating how the matching factors $\bar C$, C, and $\breve C$ match the underlying theory to effective theories where the lighter quark is described either with a Dirac field $\bar c$ or an HQET field $\bar c_{v'}$ (note subscript in HQET case); for (a) lattice gauge theory, (b) continuum QCD.

$$\bar B^{\rm lat}_{Jj} = \sum_{i=1}^{6} B^{\rm lat}_{Ji}\breve C_{Jij} + C^{\rm lat}_{J_\parallel}\breve B_{Jj}, \quad j \in S_\parallel, \tag{2.51}$$

$$\bar B^{\rm lat}_{Jj} = \sum_{i=1}^{6} B^{\rm lat}_{Ji}\breve C_{Jij} + C^{\rm lat}_{J_\perp}\breve B_{Jj}, \quad j \in S_\perp. \tag{2.52}$$

The same relations hold for the coefficients describing continuum QCD, i.e., dropping the superscript "lat". The same coefficients $\breve C$ and $\breve B$ appear, because no lattice fields appear in Eqs. (2.45)–(2.47). In Fig. 2, the bottom sides of the triangles are oblivious to the underlying theory, be it lattice gauge theory or continuum QCD. Thus, one can eliminate the $\breve C_J$ from Eqs. (2.48)–(2.50) in favor of $\bar C/C$, yielding relations between the matching factors, when $m_c a \ll 1$,

$$\bar Z_{J_\parallel} = Z_{J_\parallel}, \tag{2.53}$$

$$\bar Z_{J_\perp} = Z_{J_\perp}, \tag{2.54}$$

$$\bar Z_{J_\perp}\bar C^{\rm lat}_{J_{v'}} = \bar C_{J_{v'}}. \tag{2.55}$$

In particular, Eqs. (2.53) and (2.54) show that the heavy-heavy matching factors $\bar Z_{J_\parallel}$ and $\bar Z_{J_\perp}$ are a natural extension, into the regime $m_c a \not\ll 1$, of the heavy-light matching factors $Z_{J_\parallel}$ and $Z_{J_\perp}$. Consequently, in the following sections we shall drop the distinction and omit the bar for the heavy-heavy matching factors.

One also finds relations among the coefficients of dimension-four currents:

$$\bar Z_{J_\parallel}\bar B^{\rm lat}_{Jj} - \bar B_{Jj} = \sum_{i=1}^{6}(Z_{J_\parallel}B^{\rm lat}_{Ji} - B_{Ji})\breve C_{Jij}, \quad j \in S_\parallel, \tag{2.56}$$

$$\bar Z_{J_\perp}\bar B^{\rm lat}_{Jj} - \bar B_{Jj} = \sum_{i=1}^{6}(Z_{J_\perp}B^{\rm lat}_{Ji} - B_{Ji})\breve C_{Jij}, \quad j \in S_\perp. \tag{2.57}$$

The terms on the right-hand sides are proportional to mismatches in the heavy-light HQET. Each $Z_J B^{\rm lat}_{Ji} - B_{Ji}$ is suppressed by a power of a, multiplied by a function of $m_b a$. Similar constraints can be derived for higher-dimension coefficients. Following this reasoning for the

whole tower of higher dimension operators leads to the conclusion that, when $m_c a \ll 1$, the mismatch of the heavy-"heavy" currents reduces to that of the heavy-"light" case. In this way, lattice gauge theory reproduces the entire $1/m_c$ expansion, apart from deviations that are suppressed by powers of the other short distances, a and $1/m_b$.

Deep in the $a \to 0$ limit, where $m_c a \le m_b a \ll 1$ one can relate the short-distance coefficients of the HQET formalism to those in the Symanzik formalism.[3] For simplicity let us take $v = v'$. For the [axial] vector current, one inserts Eq. (2.12) [Eq. (2.28)] into Eq. (2.5) [Eq. (2.6)] of Ref. [2], neglects terms of order $m^2 a^2$, and compares with Eq. (2.37) [Eq. (2.38)]. One also must match the tensor bilinear to HQET at the dimension-three level,

$$\bar{c} i\sigma^{\mu\nu} b \doteq \bar{C}_T \eta^\mu_\alpha \eta^\nu_\beta \bar{c}_v i\sigma^{\alpha\beta} b_v + \cdots, \tag{2.58}$$

where one introduces another short-distance coefficient $\bar{C}_T$. At the tree level, $\bar{C}_T^{[0]} = 1$. The pseudoscalar bilinear is described by HQET operators of dimension four and higher, because $P_+(v)\gamma_5 P_+(v) = 0$. After carrying out these steps, one finds that

$$\bar{Z}_{V_\parallel} = Z_V, \tag{2.59}$$

$$\bar{Z}_{V_\parallel} \bar{B}^{\rm lat}_{Vi} = \bar{B}_{Vi} + a Z_V K_V \bar{C}_T, \quad i = 2, 6, \tag{2.60}$$

$$\bar{Z}_{V_\parallel} \bar{B}^{\rm lat}_{Vi} = \bar{B}_{V3} - a Z_V K_V \bar{C}_T, \quad i = 3, 5, \tag{2.61}$$

from matching the vector current (with Z_V and K_V as defined in Ref. [2]), and

$$\bar{Z}_{A_\perp} = Z_A, \tag{2.62}$$

$$\bar{Z}_{A_\perp} \bar{B}^{\rm lat}_{Ai} = \bar{B}_{Ai} + O(a^2), \quad i = 1, 4, \tag{2.63}$$

from matching the axial vector current (with Z_A as defined in Ref. [2]). Consequently, one sees

$$\lim_{a\to 0} \bar{Z}_{Ji} \bar{B}^{\rm lat}_{Ji} = \bar{B}_{Ji}, \tag{2.64}$$

and the limit is accelerated for standard $O(a)$ improvement. Similar relations apply for the short-distance coefficients of HQET currents of dimension five and higher.

Let us summarize the main results of this section. We have given a description of heavy-heavy lattice currents in HQET, which parallels the description of continuum QCD. The parallel structure shows that cutoff effects are isolated into the mismatch of short-distance coefficients for lattice gauge theory and continuum QCD, Eqs. (2.44) and (2.43). If the lattice currents (and Lagrangian) have enough free parameters, one can reduce the mismatch and, in this way, bring lattice calculations closer to continuum QCD, term by term in the heavy-quark expansion. In the practical region for the charmed quark, $m_c a \sim \frac{1}{3}$, it is also worth remarking that (for Wilson fermions) one could also apply the heavy-light formalism of our

---

[3] One must, of course, take the same lattice currents. The improved currents of Ref. [9] and of Sec. III are *not* the same.

companion paper [2]. Then one sees, extending Eqs. (2.56) and (2.57) to higher dimension, how the whole heavy-quark expansion for a quark with mass $m_c a < 1$ is recovered.

The remainder of this paper pursues the program of HQET matching in perturbation theory. One-loop corrections to the rest mass m_1 and the kinetic mass m_2 have been considered already in Ref. [33]. We construct lattice currents suitable for matching through dimension-five operators in the Lagrangian and dimension-four in the currents. Our heavy-heavy lattice currents turn out to be nearly the same as our heavy-light lattice currents. We then calculate the matching factors $Z_{V_\parallel}$ and $Z_{A_\perp}$ at the one-loop level, which are needed to fix the overall normalization of the heavy-light currents.

III. LATTICE ACTION AND CURRENTS

In this section our aim is to define heavy-heavy currents with Wilson fermions that are suited to the HQET matching formalism. Our construction is similar to that for heavy-light currents [2]. The descriptive part of the HQET formalism applies as long as the lattice theory has the right particle content and obeys the heavy-quark symmetries, as it does with Wilson fermions. To use HQET systematically to improve lattice gauge theory, however, one should make choices to ensure that $\delta\mathcal{C}_i$ and $\delta\bar{B}_{Ji}$ [cf. Eqs. (2.43) and (2.44)] remain bounded in the infinite-mass limit. For convenience we focus on the case when $v' = v$. Then good behavior is attained by mimicking the structure of Eqs. (2.13)–(2.18), and free parameters in the currents can be adjusted so that $\delta\mathcal{C}_i$ and $\delta\bar{B}_{Ji}$ (approximately) vanish. We show how to do so in perturbation theory, obtaining $\bar{B}^{\rm lat}_{Ji}$ at the tree level and, in Sec. IV, the matching factors $Z_{V_\parallel}$ and $Z_{A_\perp}$ at the one-loop level.

A suitable lattice Lagrangian was introduced in Ref. [4] and reviewed in the context of HQET matching in our companion paper on heavy-light currents [2]. We will not repeat the formulas here, but refer the reader to Ref. [2]. It is enough to recall that the Lagrangian has several couplings—r_s, ζ, c_B and c_E. The coupling r_s is redundant, in the technical sense, but the others can be tuned to match lattice gauge theory to continuum QCD; in this way they become non-trivial functions of the heavy quark's bare mass $m_0 a$ [4]. In particular, one may define the renormalized heavy quark mass by identifying $\mathcal{C}_2^{\rm lat} = \mathcal{C}_2$, and one can adjust c_B so that $\mathcal{C}_{\mathcal{B}}^{\rm lat} = \mathcal{C}_{\mathcal{B}}$. (If one also requires $m_1 = m_2$, one can adjust both ζ and the bare mass [4,35].)

The corresponding currents for transitions from one heavy fermion to another are defined as follows. First define a "rotated" field [12,4]

$$\Psi_q = [1 + a d_{1q} \boldsymbol{\gamma}\cdot\boldsymbol{D}_{\rm lat}]\,\psi_q, \tag{3.1}$$

where ψ_q is the field in $\mathcal{L}_0$ of flavor q ($q = c, b$), and $D_{\rm lat}$ is the symmetric covariant difference operator. (The lattice Lagrangian $\mathcal{L}_0$ is given in Eq. (3.1) of Ref. [2].) The bilinears

$$V_0^\mu = \bar{\Psi}_c i\gamma^\mu \Psi_b, \tag{3.2}$$

$$A_0^\mu = \bar{\Psi}_c i\gamma^\mu\gamma_5 \Psi_b. \tag{3.3}$$

have the correct quantum numbers, but not enough freedom to match at the dimension-four level of HQET. Thus, these currents must be improved. We focus on matching with $v' = v$, so we take

$$V^\mu_{\rm lat} = V^\mu_0 - \sum_{i\in\{2,3,5,6\}} b_{Vi} Q^\mu_{Vi}, \tag{3.4}$$

$$A^\mu_{\rm lat} = A^\mu_0 - \sum_{i\in\{1,4\}} b_{Ai} Q^\mu_{Ai}, \tag{3.5}$$

where the b_{Ji} are adjustable, and the higher-dimension lattice operators are

$$Q^\mu_{V2} = \bar\psi_c i\gamma^\mu_\perp \not{D}_{\perp\,\rm lat}\psi_b, \tag{3.6}$$

$$Q^\mu_{V3} = \bar\psi_c i D^\mu_{\perp\,\rm lat}\psi_b, \tag{3.7}$$

$$Q^\mu_{V5} = \bar\psi_c \overleftarrow{\not{D}}_{\perp\,\rm lat} i\gamma^\mu_\perp \psi_b, \tag{3.8}$$

$$Q^\mu_{V6} = \bar\psi_c i \overleftarrow{D}^\mu_{\perp\,\rm lat}\psi_b, \tag{3.9}$$

and

$$Q^\mu_{A1} = -v^\mu \bar\psi_c i\not{v}\gamma_5 \not{D}_{\perp\,\rm lat}\psi_b, \tag{3.10}$$

$$Q^\mu_{A4} = +v^\mu \bar\psi_c \overleftarrow{\not{D}}_{\perp\,\rm lat} i\not{v}\gamma_5\psi_b. \tag{3.11}$$

Lattice quark fields do not satisfy Eq. (2.2), so $\not{v}$ appears explicitly. The dimension-four lattice operators Q^μ_{Ji} are the same as for heavy-light currents, but now only corrections orthogonal (parallel) to v for the vector (axial vector) current are needed. An analogous construction for lattice NRQCD has been given by Boyle and Davies [32], who found the same pattern of dimension-four terms.

It is worth emphasizing the difference between Eq. (2.37), the corresponding equation for heavy-light currents (Eq. (2.40) of Ref. [2]), and Eq. (3.4). Equation (2.37) is a general HQET description of any heavy-heavy lattice current. Equation (3.4) is a definition of a specific lattice current, namely the one used in this paper (and in calculations of $B \to D^{(*)}$ transition matrix elements). In the same vein, the $\bar{\mathcal{Q}}_{Ji}$ in Eqs. (2.13)–(2.26) are HQET operators, whereas the Q_{Ji} in Eqs. (3.6)–(3.11) are lattice operators. Correspondingly, the coefficients $\bar B^{\rm lat}_{Ji}$ are the output of a matching calculation: they depend on the b_{Ji}, which must be adjusted to make $\delta\bar B_{Ji}$ vanish. The difference between B_{Ji} and $\mathcal{Q}_{Ji}$ ($i = 1,\ldots,6$) from Ref. [2] on the one hand, and $\bar B_{Ji}$ and $\bar{\mathcal{Q}}_{Ji}$ ($i = 1,\ldots,14$) on the other, was discussed above. In the former, the light(er) quark is described by a Dirac field; in the latter, the lighter (heavy) quark is described by an HQET field.

The difference between the definition of the lattice currents and the description with HQET can be illustrated by giving the matching coefficients at the tree level. A simple calculation of the on-shell matrix elements $\langle c|J^\mu_{\rm lat}|b\rangle$ yields

$$\bar C^{\rm lat[0]}_{V_\parallel} = e^{-(m^{[0]}_{1q}+m^{[0]}_{1b})a/2}, \tag{3.12}$$

$$\bar B^{\rm lat[0]}_{V2} = e^{-(m^{[0]}_{1q}+m^{[0]}_{1b})a/2}\left(\frac{1}{2m^{[0]}_{3b}} + b^{[0]}_{V2}\right), \tag{3.13}$$

$$\bar B^{\rm lat[0]}_{V5} = e^{-(m^{[0]}_{1q}+m^{[0]}_{1b})a/2}\left(\frac{1}{2m^{[0]}_{3c}} + b^{[0]}_{V5}\right), \tag{3.14}$$

$$\bar B^{\rm lat[0]}_{Vi} = e^{-(m^{[0]}_{1q}+m^{[0]}_{1b})a/2} b^{[0]}_{Vi}, \quad i = 3, 6, \tag{3.15}$$

for the vector current, and

$$\bar{C}_{A_\perp}^{\mathrm{lat}[0]} = e^{-(m_{1q}^{[0]}+m_{1b}^{[0]})a/2}, \tag{3.16}$$

$$\bar{B}_{A1}^{\mathrm{lat}[0]} = +e^{-(m_{1q}^{[0]}+m_{1b}^{[0]})a/2}\left(\frac{1}{2m_{3b}^{[0]}} + b_{A1}^{[0]}\right), \tag{3.17}$$

$$\bar{B}_{A4}^{\mathrm{lat}[0]} = -e^{-(m_{1q}^{[0]}+m_{1b}^{[0]})a/2}\left(\frac{1}{2m_{3c}^{[0]}} + b_{A4}^{[0]}\right), \tag{3.18}$$

for the axial vector current. The exponentials here contain the tree-level rest mass

$$m_{1h}^{[0]}a = \log(1 + m_{0h}a), \tag{3.19}$$

which enters through the wave-function normalization. The easiest way to derive these results is to combine the Feynman rule for the current in Appendix A with the Feynman rules for external lines in Appendix C of Ref. [4], and expand the matrix element $\langle c(\boldsymbol{p}')|J_{\mathrm{lat}}^{\mu}|b(\boldsymbol{p})\rangle$ to first order in $\boldsymbol{p}$ and $\boldsymbol{p}'$. The zeroth order yields the $\bar{C}$ coefficients, and the first order the $\bar{B}$ coefficients with, for our lattice Lagrangian and currents,

$$\frac{1}{2m_{3h}^{[0]}a} = \frac{\zeta(1 + m_{0h}a)}{m_{0h}a(2 + m_{0h}a)} - d_{1h} \tag{3.20}$$

for each flavor h.

One should compare Eqs. (3.12)–(3.18) with Eqs. (2.32)–(2.34). The results for $\bar{C}_{V_\parallel}^{\mathrm{lat}[0]}$ and $\bar{C}_{A_\perp}^{\mathrm{lat}[0]}$, together with $\bar{C}_{V_\parallel}^{[0]} = \bar{C}_{A_\perp}^{[0]} = 1$, show that $Z_{V_\parallel}^{[0]} = Z_{A_\perp}^{[0]} = e^{(m_{1c}^{[0]}+m_{1b}^{[0]})a/2}$. [Recall, in view of Eqs. (2.53) and (2.54), that we drop the bars from Z_J.] To obtain $\delta\bar{B}_{Ji}^{[0]} = 0$, one adjusts d_1 and the b_{Ji}. The way to adjust d_1, at the tree level, is to set $m_3^{[0]}$ equal to the (tree-level) heavy-quark mass. Since the rest mass plays only a trivial role in heavy-quark physics, the appropriate (tree-level) matching condition is $m_3^{[0]} = m_2^{[0]}$, which implies

$$d_1 = \frac{\zeta(1 + m_0a - \zeta)}{m_0a(2 + m_0a)} - \frac{r_s\zeta}{2(1 + m_0a)}. \tag{3.21}$$

If d_1 is adjusted in this way, one can then take all $b_{Ji}^{[0]} = 0$.

Beyond the tree level, it is convenient to define d_1 so that spatial component of the degenerate-mass vector current is correctly normalized. Then Q_{V2} and Q_{V5} would be superfluous for equal mass, although for unequal masses both are still needed. For the axial current Q_{A1} and Q_{A4} are required even for equal masses.

For equal-mass currents it is possible to compute $Z_{V_\parallel}^{hh}$ nonperturbatively for all m_ha. One may therefore prefer to write

$$Z_{Jcb} = \sqrt{Z_{V_\parallel}^{cc}Z_{V_\parallel}^{bb}}\rho_{Jcb} \tag{3.22}$$

and compute only the factor ρ_{Jcb} in perturbation theory. This split is very useful in numerical calculations of matrix elements [13–15]. The strong mass dependence of the Z_Js cancels, as do the contributions of tadpole diagrams: both enter through the self energy,

which is common to all Z_J factors. Hence, the expansion coefficients for ρ_J are expected to be small, and, as a consequence, the uncertainty in ρ_J from truncating perturbation theory at fixed order is under better control than the uncertainty in the corresponding Z_J. The one-loop calculation of $Z^{[1]}_{V_\parallel^{hh}}$ is given in Sec. IV B. It has been used in Ref. [2] to obtain analogous ρ_J factors for heavy-light currents. For both heavy-heavy and heavy-light currents our calculations verify that, generically, the one-loop terms $\rho_J^{[1]}$ are smaller than the corresponding $Z_J^{[1]}$.

IV. ONE-LOOP RESULTS

In this section we present results for the matching factors at the one-loop level in perturbation theory. For the Wilson and Sheikholeslami-Wohlert (SW) actions, the one-loop contributions were given in Ref. [16]. At that stage we omitted the rotation term in the current, which is needed to match dimension-four currents at the tree level [12,4]. Now we complete the work started in Ref. [16] and report results with the rotation. For comparison we also present our results without the rotation, both with and without the clover term. After some general remarks in Sec. IV A, we present numerical results for the one-loop terms. To illustrate the general features, we present three special cases: equal initial- and final-state masses in Sec. IV B, unequal masses with a fixed mass ratio in Secs. IV C, and unequal masses with a fixed final-state mass in Sec. IV D.

In the appendices, we present expressions for the Feynman rules and one-loop integrands, allowing both flavors of heavy quarks to have independent and arbitrary values of all couplings. A computer code for generating these results is freely available [19].

A. General remarks

We shall apply the formalism of Sec. II with $v' = v = (i, \mathbf{0})$, which applies when the initial and final states are at rest, or nearly at rest. The matching factors $Z_{V_\parallel}$ and $Z_{A_\perp}$ are simply ratios of the lattice and continuum radiative corrections:

$$Z_J = \frac{\left[Z_{2b}^{1/2} \Lambda_J Z_{2c}^{1/2}\right]^{\rm cont}}{\left[Z_{2b}^{1/2} \Lambda_J Z_{2c}^{1/2}\right]^{\rm lat}}, \tag{4.1}$$

where Z_{2b} and Z_{2c} are wave-function renormalization factors of the heavy bottom and charmed quarks. [Recall, in view of Eqs. (2.53) and (2.54), that we drop the bars from Z_J.] The vertex function Λ_J is the sum of one-particle irreducible three-point diagrams, in which one point comes from the current J ($J = V_\parallel$, $A_\perp$), and the other two from the external quark states. The expression relating Z_2 to the lattice self energy, for all masses and gauge couplings, can be found in Ref. [33]. In view of the mass dependence of the self-energy function, $Z_2 \propto e^{-m_1 a}$, we write

$$e^{-(m_{1c}^{[0]} a + m_{1b}^{[0]} a)/2} Z_J = 1 + \sum_{l=1}^{\infty} g^{2l} Z_J^{[l]}, \tag{4.2}$$

so that the $Z_J^{[l]}$ are only mildly mass dependent. (This convention follows that of Ref. [2], but is slightly different from the one in Ref. [33].) By construction, the exponential mass dependence in ρ_J cancels out, so we write

$$\rho_J = 1 + \sum_{l=1}^{\infty} g_0^{2l} \rho_J^{[l]}. \tag{4.3}$$

In each of the following subsections we also present the information needed to obtain the BLM scale [17,18]. Because the ideas behind the BLM prescription are covered in our paper on heavy-light currents [2], we give only the essential formulas here. Let $\zeta^{[1]}$ be one of our one-loop terms. From the Feynman diagram, it is expressed as

$$\zeta^{[1]} = \int d^4k \, f(k), \tag{4.4}$$

where k is the gluon's momentum. The BLM scale q^* is given through

$$\ln(q^* a)^2 = {}^*\zeta^{[1]}/\zeta^{[1]}. \tag{4.5}$$

where

$${}^*\zeta^{[1]} = \int d^4k \, \ln(ka)^2 \, f(k). \tag{4.6}$$

Studies of perturbation theory indicate that using $g_V^2(q^*)$ an expansion parameter usually leads to well-behaved series, because the BLM prescription pulls in some of the higher orders. Here V denotes the scheme for which the heavy-quark potential is $V(q) = -C_F g_V^2(q)/q^2$. In other schemes the optimal scale is slightly different, so that $g_S^2(q_S^*) \approx g_V^2(q^*)$.

It is also interesting to see how q^* changes under tadpole improvement. If one introduces the tadpole-improved matching factors

$$\tilde{Z}_J = Z_J/u_0, \tag{4.7}$$

where the mean link u_0 is any tadpole-dominated short-distance quantity, the arguments of Ref. [18] suggest that the perturbative series for $\tilde{Z}_J$ has smaller coefficients. In analogy with Eq. (4.2) we write

$$e^{-(\tilde{m}_{1c}^{[0]} + \tilde{m}_{1b}^{[0]})a/2} \tilde{Z}_J = 1 + \sum_{l=1}^{\infty} g_0^{2l} \tilde{Z}_J^{[l]}, \tag{4.8}$$

where

$$\tilde{m}_1^{[0]} a = \ln[1 + m_0 a/u_0] \tag{4.9}$$

is the tadpole-improved rest mass. Then

$$\tilde{Z}_J^{[1]} = Z_J^{[1]} - \frac{1}{2}\left(\frac{1}{1 + m_{0c}a} + \frac{1}{1 + m_{0b}a}\right) u_0^{[1]}, \tag{4.10}$$

and because $Z_J^{[1]} < 0$ and $u_0^{[1]} < 0$ one sees that the one-loop coefficients are reduced. Similarly, for computing the BLM scale

$$ {}^*\tilde{Z}_J^{[1]} = {}^*Z_J^{[1]} - \frac{1}{2}\left(\frac{1}{1+m_{0c}a} + \frac{1}{1+m_{0b}a}\right) {}^*u_0^{[1]}. \tag{4.11} $$

To illustrate, we take u_0 from the average plaquette, so $u_0^{[1]} = -C_F/16$ and ${}^*u_0^{[1]} = -0.204049(1)$.

The combinations of wave-function and vertex renormalization in Z_J are gauge invariant and ultraviolet and infrared finite. Infrared cancellation between lattice and continuum integrands occurs point-by-point if the masses in continuum propagators are set equal to the corresponding kinetic masses. Because there are no divergences, it is straightforward to weight the integrands with $\ln(ka)^2$.

Although the main results of this section, given below, are the calculation of the full mass dependence of the one-loop terms, let us anticipate what to expect in limiting cases. When both masses vanish, we must (and do) obtain the textbook result for matching in the Symanzik formalism. If one mass vanishes, we must recover our results for heavy-light matching factors. In fact, our codes are based on the same integrand functions, so this "check" is automatic.

When both masses satisfy $m_h \gg a^{-1}$, both heavy-quark propagators become static, and, consequently, the one-loop lattice radiative corrections vanish. Thus, the matching factors reduce to the continuum QCD radiative corrections. Using Eqs. (2.29) and (2.30)

$$ \lim_{m_b a,\, m_c a \to \infty} Z_{V_\parallel}^{[1]} \to \bar{C}_{V_\parallel}^{[1]} = C_F\, 3f(m_{2c}/m_{2b})/16\pi^2, \tag{4.12} $$

$$ \lim_{m_b a,\, m_c a \to \infty} Z_{A_\perp}^{[1]} \to \bar{C}_{A_\perp}^{[1]} = C_F\left[3f(m_{2c}/m_{2b}) - 2\right]/16\pi^2. \tag{4.13} $$

The lattice contribution to the BLM numerator ${}^*\zeta^{[1]}$ also vanishes in this limit, leaving

$$ \lim_{m_b a,\, m_c a \to \infty} {}^*Z_{V_\parallel}^{[1]} \to {}^*\bar{C}_{V_\parallel}^{[1]} = C_F\, 9f(m_{2c}/m_{2b})/32\pi^2 + \bar{C}_{V_\parallel}^{[1]} \ln(m_{2b}a m_{2c}a), \tag{4.14} $$

$$ \lim_{m_b a,\, m_c a \to \infty} {}^*Z_{A_\perp}^{[1]} \to {}^*\bar{C}_{A_\perp}^{[1]} = C_F\left[\tfrac{5}{2}f(m_{2c}/m_{2b}) - 1\right]/16\pi^2 + \bar{C}_{A_\perp}^{[1]} \ln(m_{2b}a m_{2c}a), \tag{4.15} $$

where the right-hand sides are due to Ref. [36].

When one mass becomes very large, but the other is held fixed, one can still deduce the limiting behavior from Eqs. (4.12)–(4.15). As the heavier mass increases, $m_{2b}a \to \infty$, the lattice Feynman diagrams become independent of $m_{2b}a$. The logarithmic part then takes the form $3\ln(m_{2c}a)$. This lattice logarithm cancels only part of the corresponding logarithm in $3f(m_{2c}/m_{2b})$, leaving the matching factor with $3\ln(m_{2b}a)$. Then non-logarithmic constants depend, of course, on the fixed mass of the lighter quark. In the BLM numerators, for $m_{2c}a$ held fixed and $m_{2b}a \to \infty$, one obtains a quadratic in $\ln(m_{2b}a)$, in which the coefficient of $\ln^2(m_{2b}a)$ is identical to those of the continuum radiative corrections, and the coefficient of the single logarithm and the non-logarithmic term itself are mildly dependent on $m_{2c}a$.

Below we plot the mass dependence as a function of $m_{1b}^{[0]}a$, because it brings out the asymptotic behavior for both $m_h a = 0$ and $m_h a \to \infty$: when $m_h a \ll 1$, $m_{1h}^{[0]} \approx m_{2h}^{[0]}$, but when $m_h a \gg 1$, $m_{1h}^{[0]}a \approx \ln(m_{2h}^{[0]}a)$. Thus, a plot against $m_{1b}^{[0]}a$ makes it easy to look both at slope and curvature in the small-mass region, and at the expected logarithms in the large-mass region.

In presenting results below, we show together $Z_J^{[1]}$, ${}^*Z_J^{[1]}$, $\rho_J^{[1]}$, and ${}^*\rho_J^{[1]}$, for each current, followed by the BLM scale for $Z_{V_\parallel}$ and $Z_{A_\perp}$.

B. Degenerate masses

Figure 3 shows the full mass dependence of the matching factor $Z_{V_\parallel}^{[1]}$ for the vector current, with $m_{2c} = m_{2b}$, and its BLM numerator ${}^*Z_{V_\parallel}^{[1]}$. Figure 4 shows the same for the axial vector current, including the one-loop term for $\rho_{A_\perp}$ and its BLM numerator ${}^*\rho_{A_\perp}$. In this case, with equal masses, one has simply $\rho_{A_\perp} = Z_{A_\perp}/Z_{V_\parallel}$. As expected, all interpolate smoothly from small to large quark mass. Except for ${}^*\rho_{A_\perp}^{[1]}$, the curves exhibit a "knee" around $m_1^{[0]}a \sim 1$–2 ($m_0 a \approx m_2 a \sim 2$–$6$). For ${}^*\rho_{A_\perp}^{[1]}$ the knee effect seems to cancel, and the function crosses over quickly to logarithmic behavior.

For $m_c a = m_b a = 0$, our matching factors must (and do) reduce to the well-known massless limit, obtained long ago for $c_{\rm SW} = 1$ [37] and even longer ago for $c_{\rm SW} = 0$ [38]. As discussed above, in the infinite mass limit (with a fixed), the heavy-quark spin symmetry of Wilson fermions ensures that the lattice radiative corrections vanish. The infinite mass limits are $Z_{V_\parallel}^{[1]} = 0$, ${}^*Z_{V_\parallel}^{[1]} = 0$, $Z_{A_\perp}^{[1]} = \rho_{A_\perp}^{[1]} = -2C_F/16\pi^2$, and ${}^*Z_{A_\perp}^{[1]} = {}^*\rho_{A_\perp}^{[1]} = -C_F[4\ln(m_2 a) + 1]/16\pi^2$. They are shown in each panel of Figs. 3 and 4 with a dashed-dotted line. As a rule, the tendency to the infinite mass limit becomes obvious for $m_1^{[0]}a > 5$ ($m_0 a \approx m_2 a > 150$).

For smaller masses ($m_c a,\ m_b a \lesssim 1$), one expects the one-loop term $\rho_{A_\perp}^{[1]}$ to be smaller than $Z_{A_\perp}^{[1]}$, because it does not contain any tadpole diagrams. This expectation is borne out in comparing Fig. 4(a) and (c). For larger masses, the tadpole diagram is suppressed, cf. Eqs. (4.10) and (4.11), and $\rho_{A_\perp}^{[1]}$ and $Z_{A_\perp}^{[1]}$ have the same asymptotic value. By comparing Fig. 4(b) and (d), one sees that ${}^*\rho_{A_\perp}^{[1]}$ is smaller than ${}^*Z_{A_\perp}^{[1]}$ also.

In Fig. 5 we combine the information from Figs. 3 and 4 and show the BLM scale q^*a for the vector and axial vector currents. In the region of greatest interest, $m_{1b} \le 1$ ($m_{2b} < 1.5$), we find $q^*a \approx 2.8$ for the clover action. In Fig. 6 we apply tadpole improvement. In the region of greatest interest, $m_{1b} \le 1$, we find a smaller $q^*a \approx 1.8$–2.0 for the clover action. The singular behavior for $Z_{V_\parallel}$ for $m_{1b} \gtrsim 1.5$ arises because the denominator vanishes. If numerator and denominator in Eq. (4.5) have the same (opposite) sign, then $q^*a \to \infty$ ($q^*a \to 0$). In such a case the BLM prescription does not make sense and should be modified [41].

With equal masses, the matching factor $Z_{V_\parallel}$ can be computed non-perturbatively, allowing us to test how well BLM perturbation theory works. Figure 7 plots $\exp(-m_{1b}^{[0]}a)Z_{V_\parallel}$ vs. $m_{1b}^{[0]}a$ for several methods of calculating $Z_{V_\parallel}$. In perturbation theory, we truncate Eq. (4.2) at the first non-trivial term, and use either the bare coupling g_0^2 or the BLM prescription $g_V^2(q^*)$. We also truncate Eq. (4.8) at the first non-trivial term, which is tadpole improvement. As a non-perturbative check, we define

$$\frac{1}{Z_{V_\parallel}^{\rm NP}} = \frac{\langle H|\bar\Psi_b \gamma_4 \Psi_b|H\rangle}{\langle H|H\rangle} \tag{4.16}$$

where H is a b-flavored hadron. Results for several b masses at bare gauge coupling $g_0^2 = 6/5.9$ [42] are shown in Fig. 7. We also plot the Taylor expansion for small mass

$$Z_{V_\parallel}(m_0 a) = Z_V\,[1 + b_V m_0 a]\,, \tag{4.17}$$

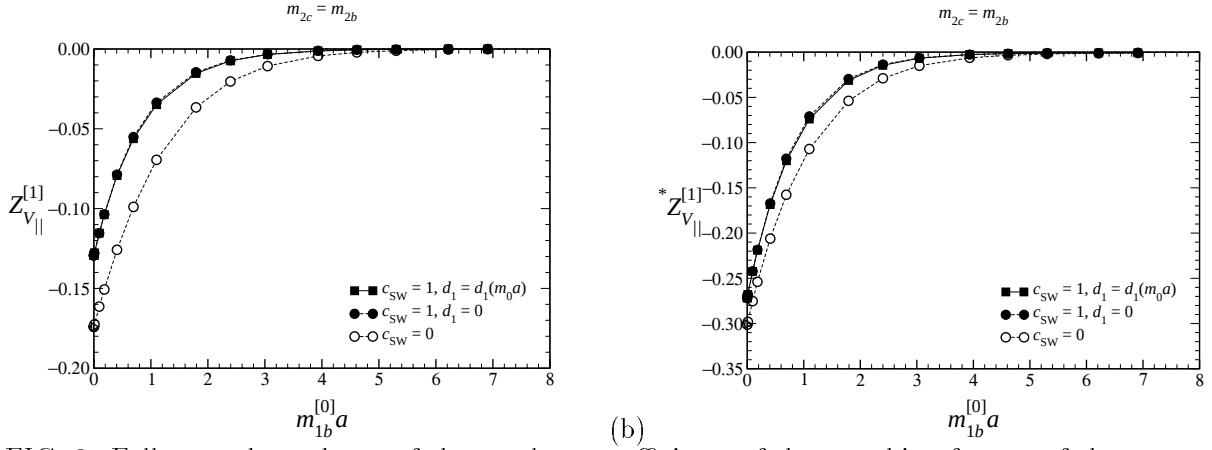

FIG. 3. Full mass dependence of the one-loop coefficients of the matching factors of the vector current with equal masses: (a) $Z^{[1]}_{V_{||}}$ and (b) $^{*}Z^{[1]}_{V_{||}}$. Filled (open) symbols denote the SW (Wilson) action. Solid (dotted) lines connecting squares (circles) indicate the rotation is included (omitted).

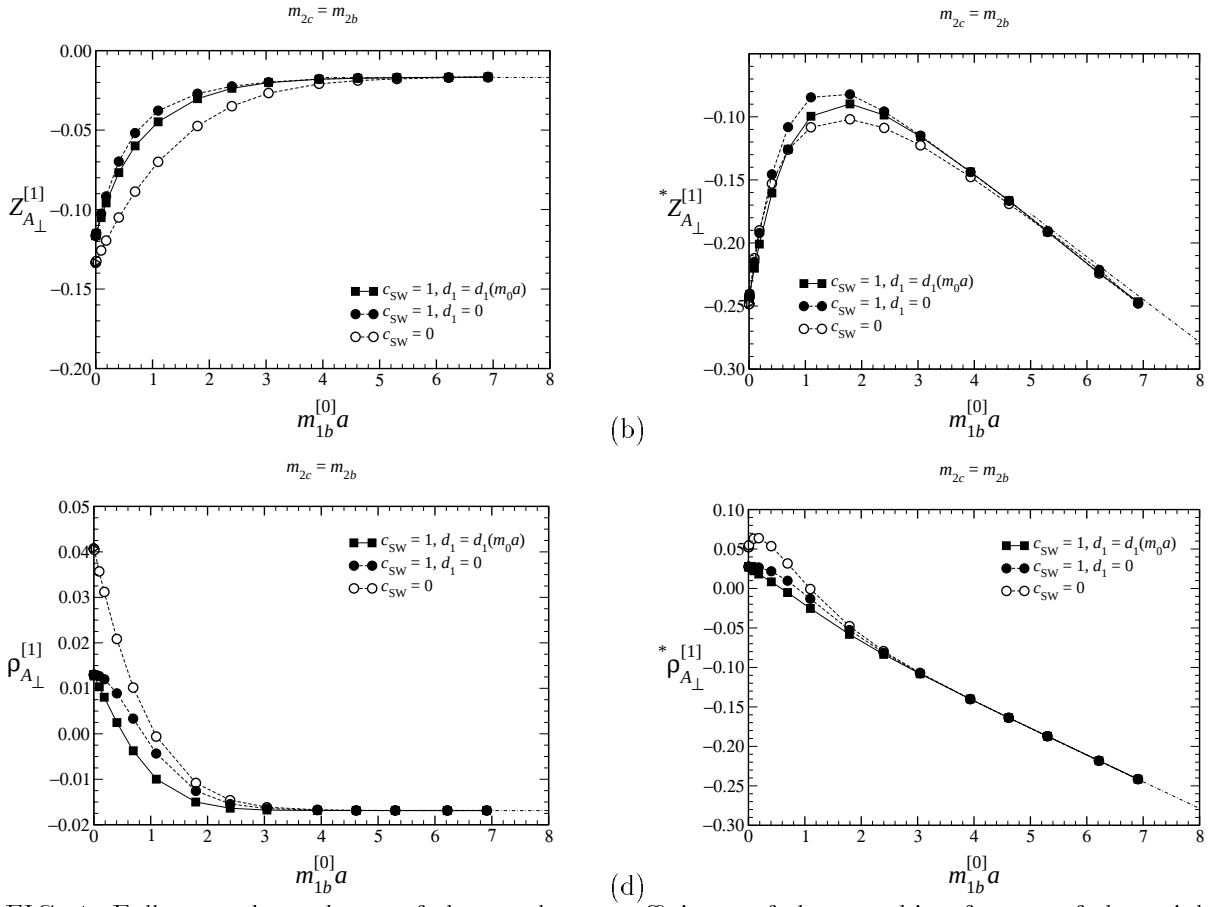

FIG. 4. Full mass dependence of the one-loop coefficients of the matching factors of the axial vector current with equal masses: (a) $Z^{[1]}_{A_\perp}$, (b) $^{*}Z^{[1]}_{A_\perp}$, (c) $\rho^{[1]}_{A_\perp}$, and (d) $^{*}\rho^{[1]}_{A_\perp}$. The symbols have the same meaning as in Fig. 3; dashed-dotted lines show the infinite-mass limit.

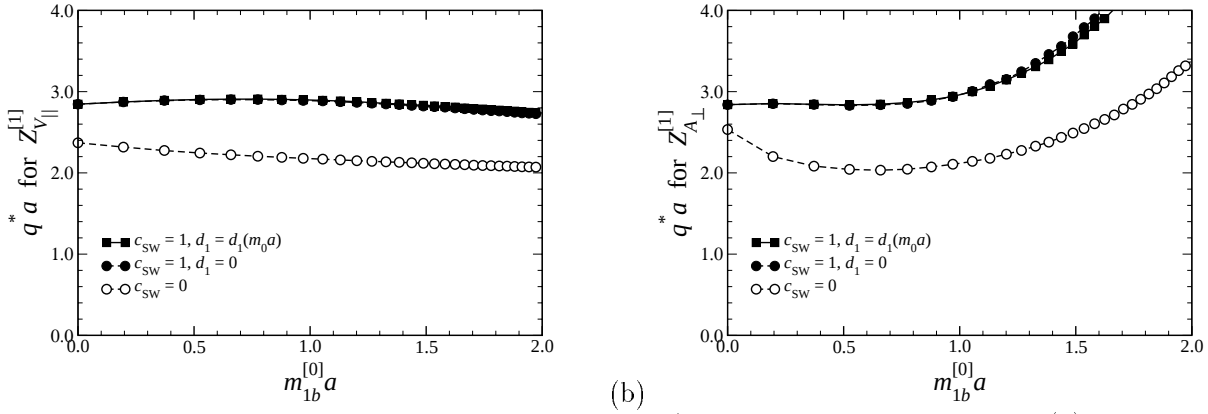

FIG. 5. Full mass dependence of the BLM scale q^*a for the matching factors (a) $Z_{V_\parallel}$ and (b) $Z_{A_\perp}$, with $m_c = m_b$. The symbols have the same meaning as in Figs. 3 and 4.

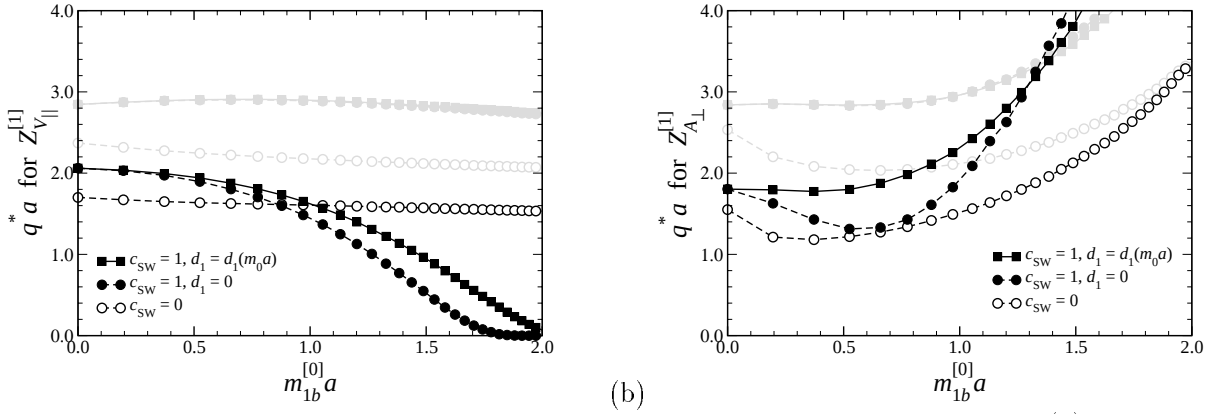

FIG. 6. Full mass dependence of the BLM scale q^*a for the matching factors (a) $Z_{V_\parallel}$ and (b) $Z_{A_\perp}$, with $m_c = m_b$, after tadpole improvement. Curves from Fig. 5 are shown in grey.

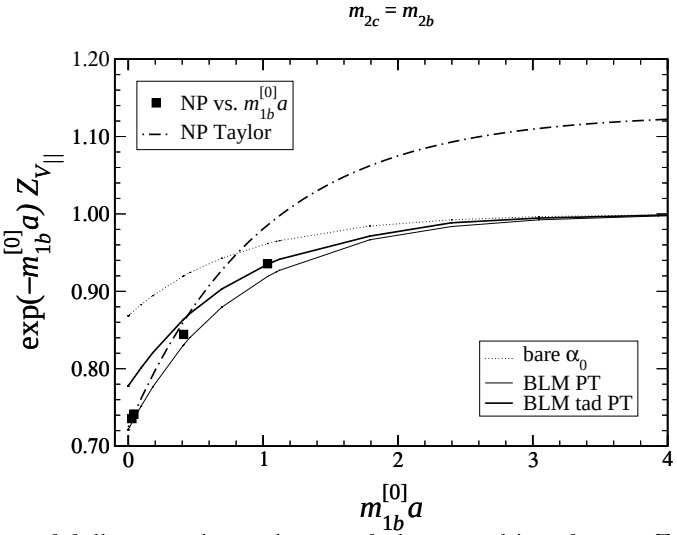

FIG. 7. Comparison of full mass dependence of the matching factor $Z_{V_\parallel}$. The symbols are a non-perturbative, hadronic calculation [42]. The dotted curve is bare perturbation theory. The solid curves are BLM perturbation theory; the heavy (light) line includes (omits) tadpole improvement. The dashed-double-dotted curve shows the first-order Taylor series, with intercept and slope determined non-perturbatively.

where the notation on the right-hand side follows Ref. [9]. From the two small-mass points, we determine $Z_V = 0.7247$ and $b_V = 1.5588$ (for $g_0^2 = 6/5.9$ and $c_{\rm SW} = 1.50$). Figure 7 reveals several lessons. First, bare perturbation theory deviates from the non-perturbative points by several percent. Second, BLM perturbation theory is quite accurate for all masses. The deviations are a few percent: they are neither completely absent nor several percent. Third, it is less accurate to neglect the full mass dependence (using only Z_V from $ma \to 0$) than to use BLM perturbation theory, already around the charmed quark mass ($m_1 \sim 0.5$). Finally, although Eq. (4.17) remains within a few percent of the full mass dependence for $m_1 \leq 0.5$ (cf. dashed-double-dotted curve), it does not have the correct large mass limit. It gives an explicit example of the pitfalls that arise in applying the improvement program of Refs. [9,10] to heavy quarks.

C. Unequal masses: fixed mass ratio

In a typical usage of the matching factors, one wants to calculate a physical process, such as $B \to D^{(*)} l\nu$. To monitor lattice spacing effects, one would like to repeat the calculation at several lattice spacings with the ratio of the initial and final heavy quark masses held fixed. It is therefore useful to see how the matching factors vary with $m_{1b}a$ at fixed $z = m_{2c}^{[0]}/m_{2b}^{[0]}$. For illustration we choose $z = 0.256$, which was used in a recent calculation [13] of the form factors for $B \to Dl\nu$.

Figure 8 shows the full mass dependence of $Z_{V_\parallel}^{[1]}$, ${}^*Z_{V_\parallel}^{[1]}$, $\rho_{V_\parallel}^{[1]}$, and ${}^*\rho_{V_\parallel}^{[1]}$, with $z = m_{2c}/m_{2b}$ held fixed at 0.256. Figure 9 shows the same for $Z_{A_\perp}^{[1]}$, ${}^*Z_{A_\perp}^{[1]}$, $\rho_{A_\perp}^{[1]}$, and ${}^*\rho_{A_\perp}^{[1]}$. The behavior is qualitatively similar to that with $z = 1$. After a knee, the expected infinite mass limit is again reached for $m_1^{[0]}a > 5$. The asymptotic behavior is shown with the dashed-dotted lines:

$$\rho_{V_\parallel}^{[1]} = Z_{V_\parallel}^{[1]} = +0.901 C_F/16\pi^2, \tag{4.18}$$

$$\rho_{A_\perp}^{[1]} = Z_{A_\perp}^{[1]} = -1.099 C_F/16\pi^2, \tag{4.19}$$

and

$${}^*\rho_{V_\parallel}^{[1]} = {}^*Z_{V_\parallel}^{[1]} = C_F[0.124 + 1.802\ln(m_2 a)]/16\pi^2, \tag{4.20}$$

$${}^*\rho_{A_\perp}^{[1]} = {}^*Z_{A_\perp}^{[1]} = C_F[1.248 - 2.198\ln(m_2 a)]/16\pi^2, \tag{4.21}$$

using $f(0.256) = 0.3003$. For both currents, the crossover in ${}^*\rho_J^{[1]}$ is smooth enough that no knee is manifest.

At the largest masses our numerical integration (with VEGAS [39] or BASES [40]) deteriorates, because ultraviolet divergences of the continuum vertex and self-energy diagrams do not cancel point by point (as they do when $z = 1$). If accurate values of the one-loop terms were essential, this numerical difficulty could be avoided. But it arises for values of $m_{1b}a$ where the quarks are essentially static, and one may just as well make them completely static.

In Fig. 10 we combine the information from Figs. 8 and 9 and show the BLM scale q^*a for the vector and axial vector currents. In the region of greatest interest, $m_{1b} \leq 1$, we find

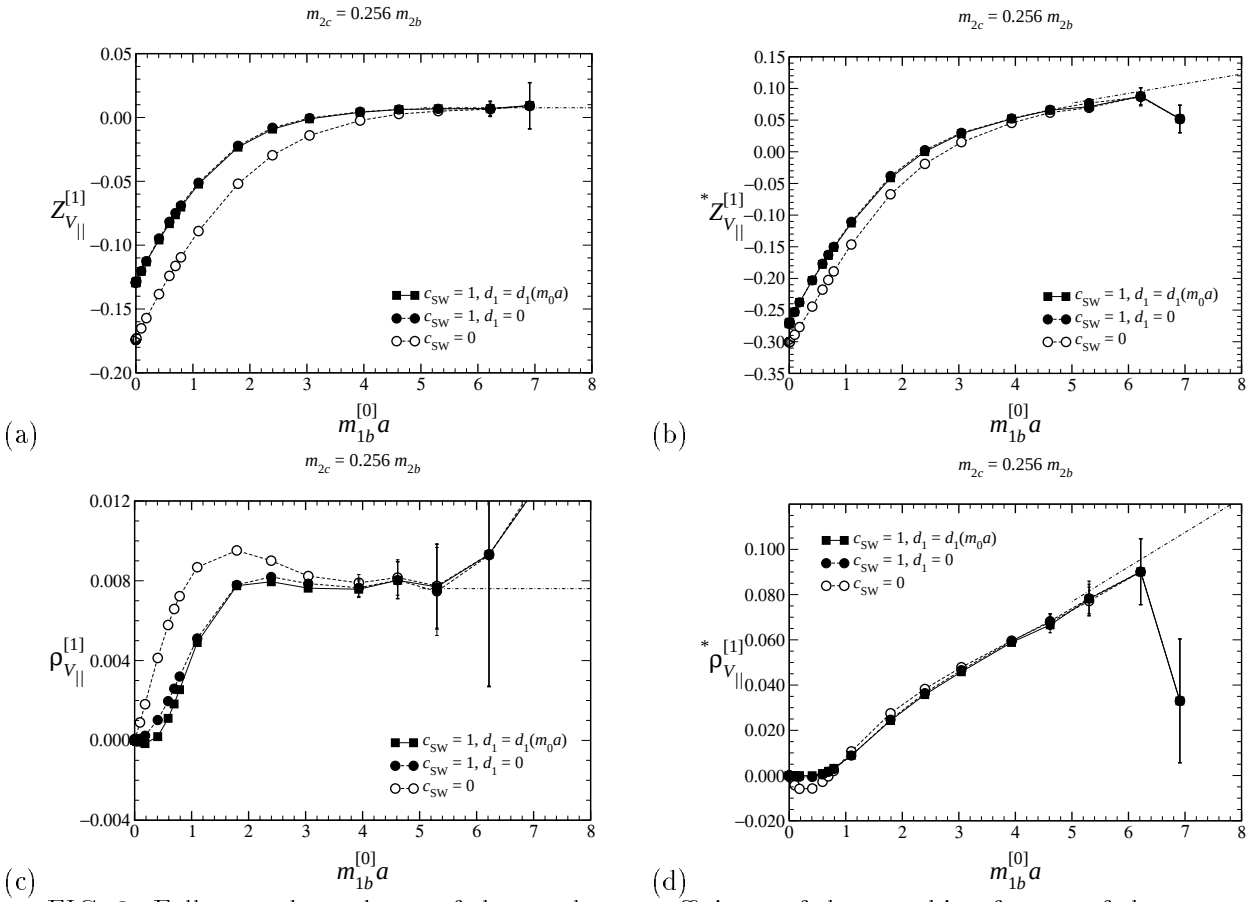

FIG. 8. Full mass dependence of the one-loop coefficients of the matching factors of the vector current with $z = 0.256$: (a) $Z^{[1]}_{V_\parallel}$, (b) ${}^*Z^{[1]}_{V_\parallel}$, (c) $\rho^{[1]}_{V_\parallel}$, and (d) ${}^*\rho^{[1]}_{V_\parallel}$. The symbols have the same meaning as in Figs. 3 and 4.

$q^*a \approx 2.8$ for the clover action. In Fig. 11 we apply tadpole improvement. In the region of greatest interest, $m_{1b} \leq 1$, we find a smaller $q^*a \approx 1.8$–2.0 for the clover action. The singular behavior for $Z_{V_\parallel}$ near $m_{1b} \sim 1.5$ (and for $Z_{A_\perp}$ near $m_{1b} \sim 2.5$) arises, again, because the denominator vanishes, so one should switch to the modified prescription of Ref. [41].

As we have mentioned above, when $m_h \gg a^{-1}$ for both flavors, heavy quark symmetries emerge [1]. One consequence is that the one-loop lattice radiative corrections vanish, as Figs. 3, 4, 8, and 9 verify numerically. There is an interesting further consequence for $\rho_{V_\parallel}$, in which the unphysical $e^{m_1 a}$ normalization drops out. Its approach to the infinite-mass limit must satisfy[4]

$$\frac{\bar{C}_{V_\parallel}}{\rho_{V_\parallel}} \equiv \bar{C}^{\rm lat}_{V_\parallel} = \Delta_2^2 \left[\bar{c}^{(2)} + \bar{c}^{(3)} \Sigma_2 \right], \tag{4.22}$$

[4]In Sec. II, $\bar{C}^{\rm lat}_{V_\parallel}$ is a generic notation for a matching coefficient in HQET. Here it denotes the same coefficient for the specific current $\sqrt{Z_{V_\parallel}^{cc} Z_{V_\parallel}^{bb}}\, \bar{\Psi}_c \gamma^4 \Psi_b$.

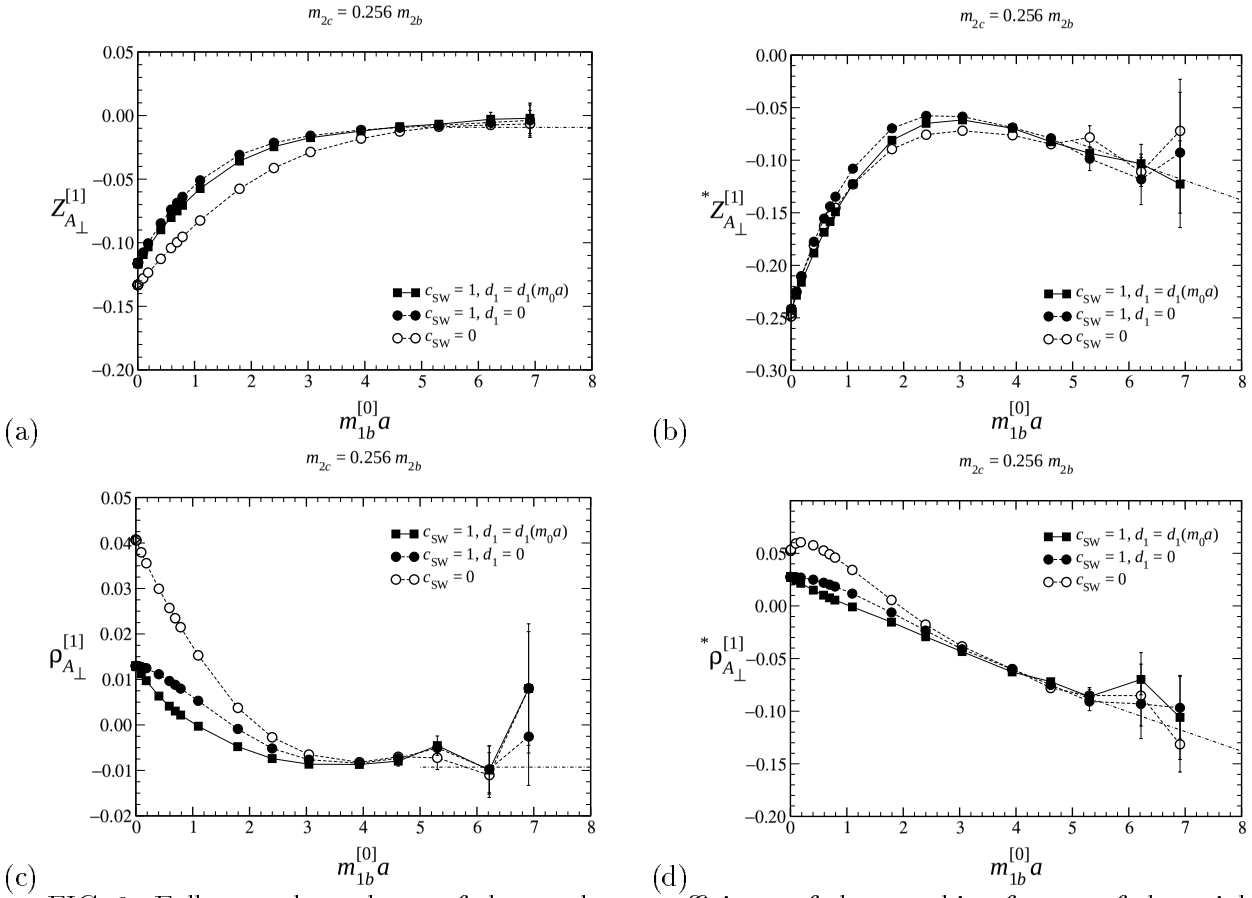

FIG. 9. Full mass dependence of the one-loop coefficients of the matching factors of the axial vector current with $z = 0.256$: (a) $Z_{A_\perp}^{[1]}$, (b) ${}^*Z_{A_\perp}^{[1]}$, (c) $\rho_{A_\perp}^{[1]}$, and (d) ${}^*\rho_{A_\perp}^{[1]}$. The symbols have the same meaning as in Figs. 3 and 4.

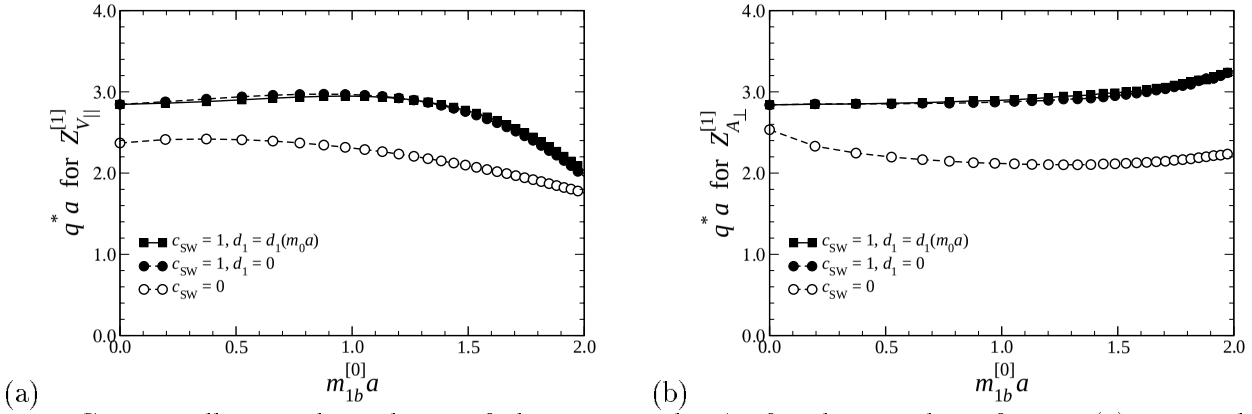

FIG. 10. Full mass dependence of the BLM scale q^*a for the matching factors (a) $Z_{V_\parallel}$ and (b) $Z_{A_\perp}$, with $m_{2c} = 0.256 m_{2b}$. The symbols have the same meaning as in Figs. 8 and 9.

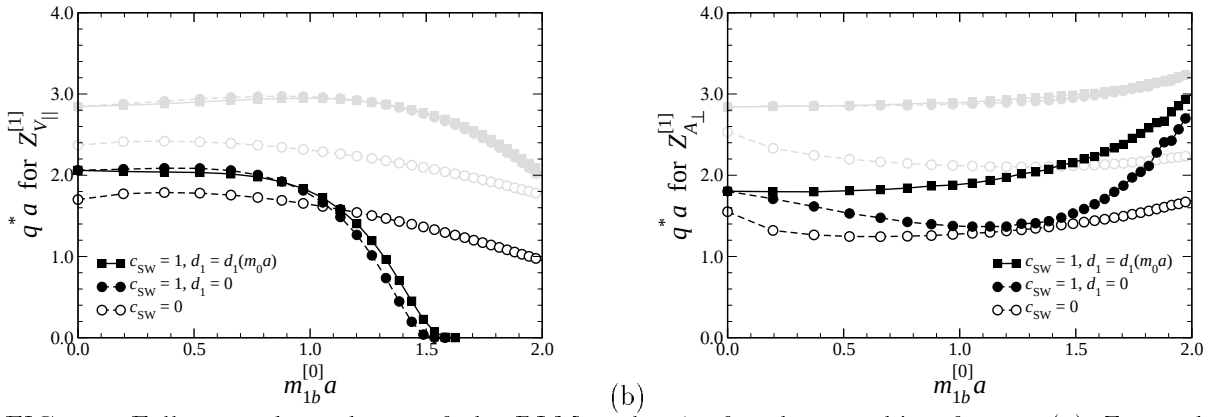

FIG. 11. Full mass dependence of the BLM scale q^*a for the matching factors (a) $Z_{V_\parallel}$ and (b) $Z_{A_\perp}$, with $m_{2c} = 0.256 m_{2b}$, after tadpole improvement. Curves from Fig. 10 are shown in grey.

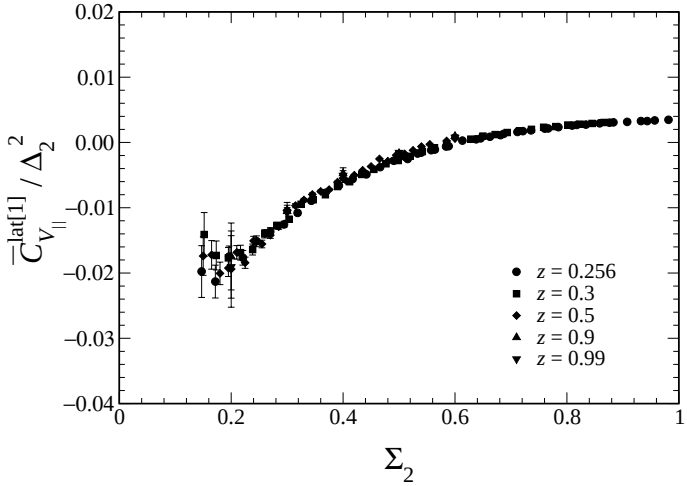

FIG. 12. Test of Luke's theorem, namely Eq. (4.22) at one loop, for several mass ratios $z = 0.256, 0.3, 0.5, 0.9, 0.99$.

where the $\bar{c}^{(n)}$ are independent of the masses, and

$$\Delta_2 = \frac{1}{2m_{2c}a} - \frac{1}{2m_{2b}a}, \tag{4.23}$$

$$\Sigma_2 = \frac{1}{2m_{2c}a} + \frac{1}{2m_{2b}a}. \tag{4.24}$$

Equation (4.22) is a version of Luke's theorem [43]. It follows because the mass dependence must be symmetric under the interchange $m_c \leftrightarrow m_b$, and because $\rho_{V_\parallel}$ must vanish when $m_c = m_b$. Following Ref. [32] we test whether our one-loop calculation satisfies the theorem for a variety of different mass ratios. Figure 12 plots $\bar{C}_{V_\parallel}^{\mathrm{lat}[1]}/\Delta_2^2$ vs. Σ_2 for $z = 0.256, 0.3, 0.5, 0.9, 0.99$. All mass combinations lie essentially on a single curve, verifying Eq. (4.22). Small deviations are possible (and noticeable in Fig. 12), arising from higher orders in the small $\boldsymbol{p}$ exapnsion of the quark propagator, where coefficients other than $1/(2m_2 a)$ appear.

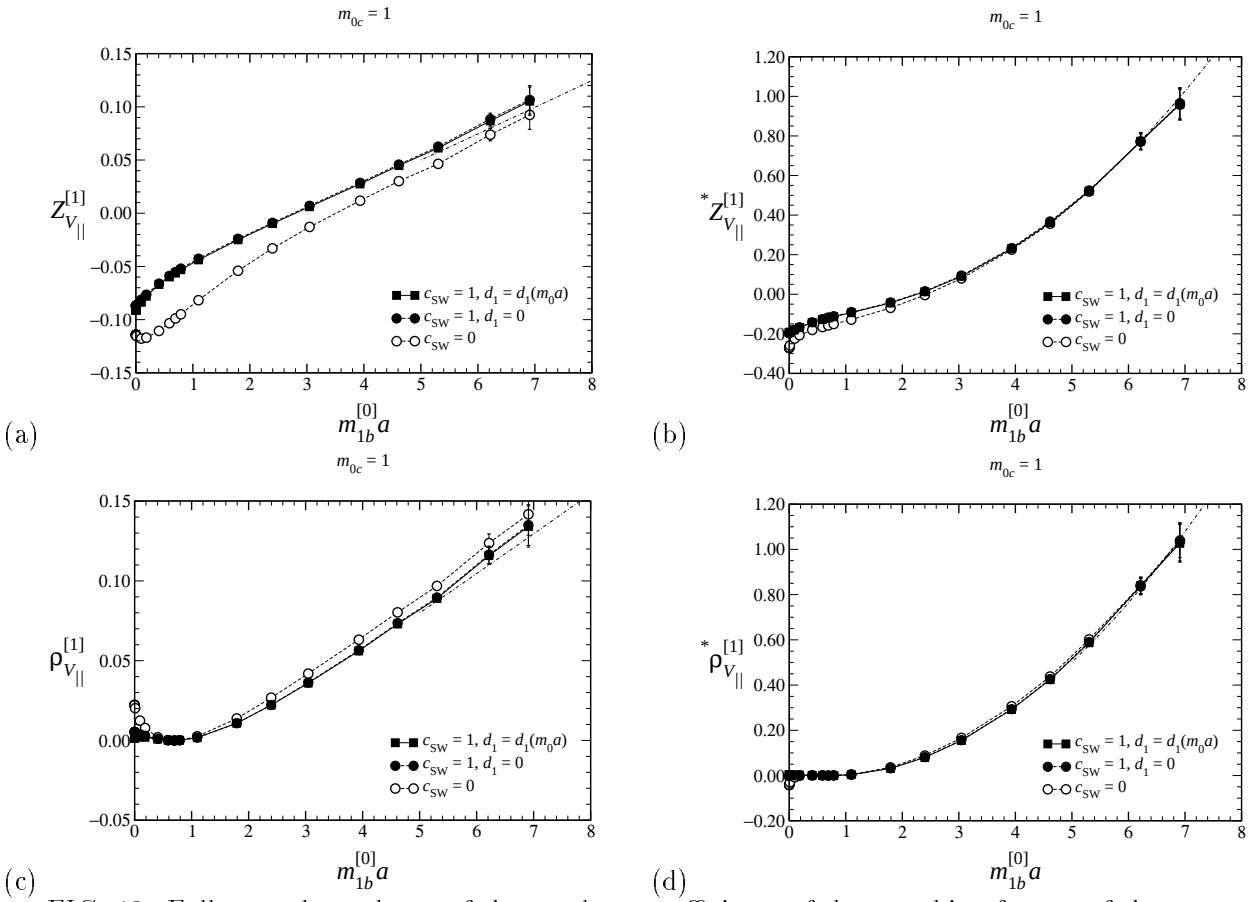

FIG. 13. Full mass dependence of the one-loop coefficients of the matching factors of the vector current with $m_{0c} = 1$: (a) $Z^{[1]}_{V_\parallel}$, (b) ${}^*Z^{[1]}_{V_\parallel}$, (c) $\rho^{[1]}_{V_\parallel}$, and (d) ${}^*\rho^{[1]}_{V_\parallel}$. The symbols have the same meaning as in Figs. 3 and 4.

D. Unequal masses: fixed daughter mass

In this subsection we study the matching factors, varying only the initial mass while holding the final mass fixed. For illustration we set $m_{0c}a = 1$. As discussed above, one expects the large-mass limit to exhibit some qualitative behavior seen in the heavy-light matching factors in our heavy-light paper [2]. Thus, looking at this slice through the function of two variables can illustrate how the heavy-heavy matching factors are an extension of the heavy-light matching factors.

Figure 13 shows full m_ba dependence of $Z^{[1]}_{V_\parallel}$, ${}^*Z^{[1]}_{V_\parallel}$, $\rho^{[1]}_{V_\parallel}$, and ${}^*\rho^{[1]}_{V_\parallel}$, with fixed $m_{0c}a = 1$ ($m_{2c}a = 0.857$). Figure 14 shows the same for $Z^{[1]}_{A_\perp}$, ${}^*Z^{[1]}_{A_\perp}$, $\rho^{[1]}_{A_\perp}$, and ${}^*\rho^{[1]}_{A_\perp}$. As with the heavy-light matching factors [2], a knee is not really visible, because soon after reaching $m^{[0]}_{1b}a \gtrsim 2$ ($m_{2b}a \gtrsim 6$), logarithmic behavior starts to dominate. For small m_ba, one finds that $\rho_{V_\parallel}(m_ba = 0, m_{0c}a = 1) \neq 0$, but with the SW action it is very small: 0.0015017(9) with the rotation on the c leg and 0.0054380(10) without.

In Fig. 15 we combine the information from Figs. 13 and 14 and show the BLM scale q^*a for the vector and axial vector currents. In the region of greatest interest, $m_{1b} \leq 1$, we find $q^*a \approx 2.8$–3.0 for the clover action (and 2.0–2.2 for the Wilson action). In Fig. 16 we

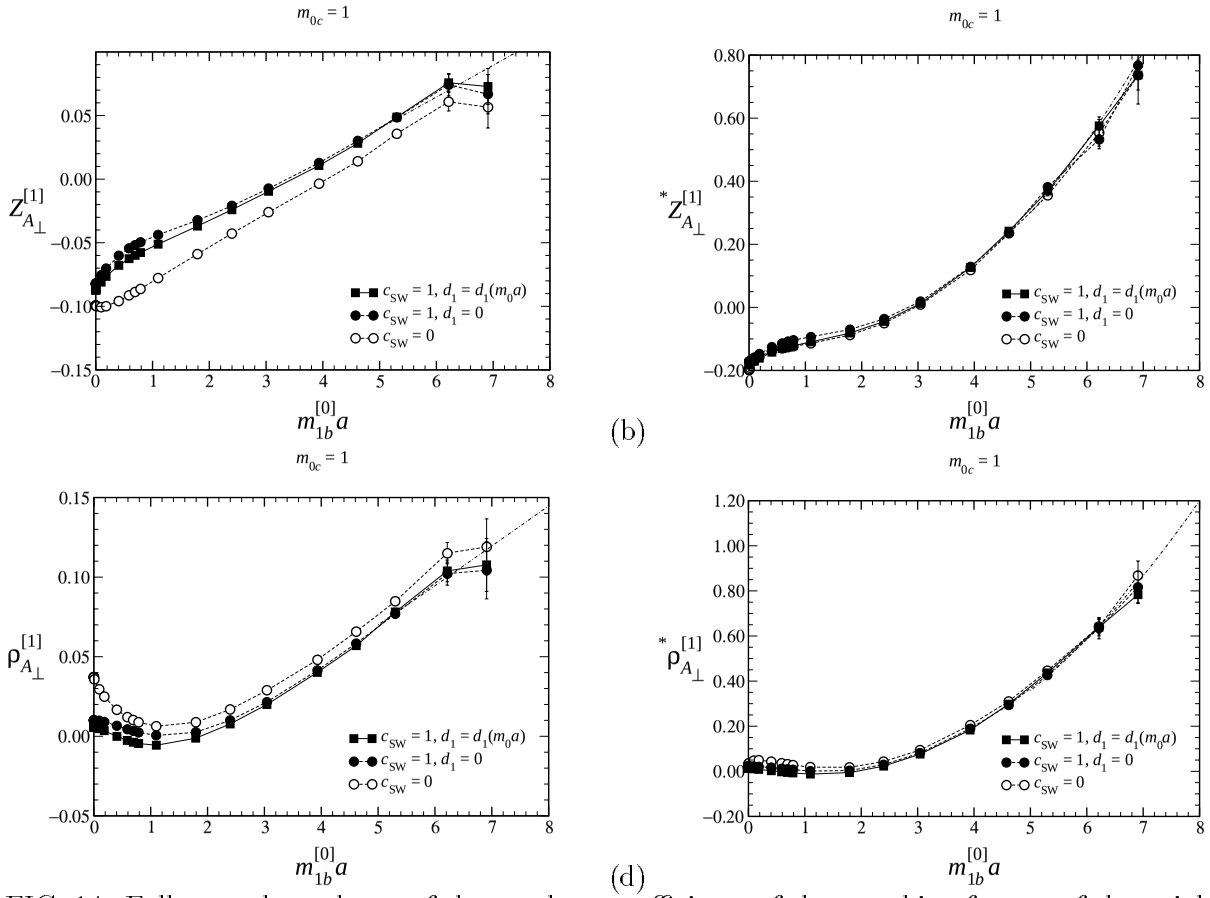

FIG. 14. Full mass dependence of the one-loop coefficients of the matching factors of the axial vector current with $m_{0c} = 1$: (a) $Z^{[1]}_{A_\perp}$, (b) ${}^*Z^{[1]}_{A_\perp}$, (c) $\rho^{[1]}_{A_\perp}$, and (d) ${}^*\rho^{[1]}_{A_\perp}$. The symbols have the same meaning as in Figs. 3 and 4.

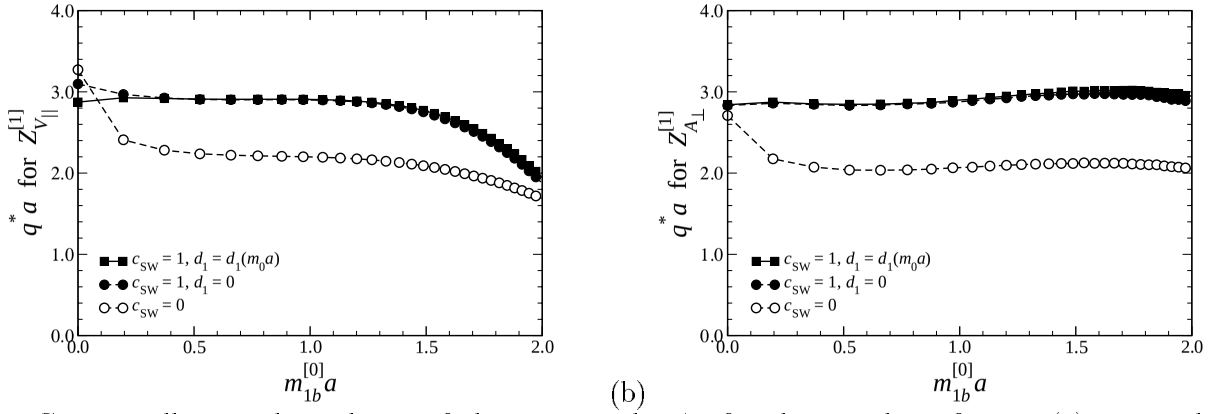

FIG. 15. Full mass dependence of the BLM scale q^*a for the matching factors (a) $Z_{V_\parallel}$ and (b) $Z_{A_\perp}$, with $m_{0c}a = 1$. The symbols have the same meaning as in Figs. 13 and 14.

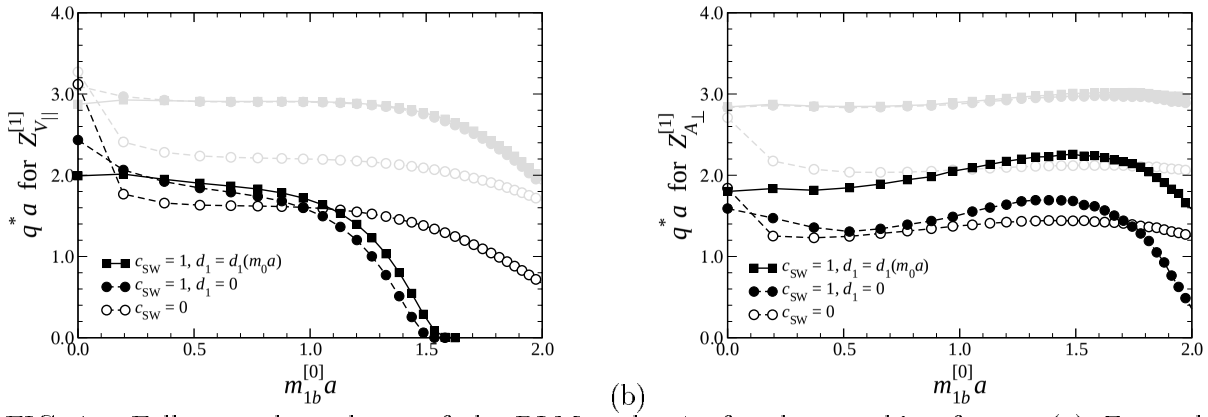

FIG. 16. Full mass dependence of the BLM scale q^*a for the matching factors (a) $Z_{V_\parallel}$ and (b) $Z_{A_\perp}$, with $m_{0c}a = 1$, after tadpole improvement. Curves from Fig. 15 are shown in grey.

apply tadpole improvement. In the region of greatest interest, $m_{1b} \leq 1$, we find a smaller $q^*a \approx 1.8$–1.0 for the clover action (and 1.2–1.4 for the Wilson action). The singular behavior for $Z_{V_\parallel}$ ($Z_{A_\perp}$) near $m_{1b} \sim 1.5$ (2.2) arises, once again, because the denominator in Eq. (4.5) vanishes, so one should switch to the modified prescription of Ref. [41].

E. Summary

Let us summarize the main points of this section. The heavy-heavy matching factors are a function of two variables, and we have plotted several one-dimensional slices to illustrate their size and behavior. The dependence on the masses smoothly connects the limit where $m_h a \ll 1$ with the infinite-mass limit(s). This is typical of radiative corrections in massive lattice gauge theory [4], and the phenomenon should, by now, be familiar from several explicit examples [44–46,33,16,47,2].

There are several checks on our calculations. Numerical results have been tested with two or more completely independent programs. The curves behave as expected for large mass. When one mass is very small in lattice units, our results smoothly connect to the heavy-light matching factors. When both are small we reproduce results in the literature for massless fermions. We are confident, therefore, that our programs compute the one-loop coefficients correctly for intermediate values of the masses.

It does not seem especially useful to print tables of our results. In practice [13,14], one will want to analyze many different mass combinations. To facilitate this analysis, we are making one suite of programs freely available [19]. That will allow the user to obtain the coefficients to suit his or her needs. As shown in Appendix B we have found a way to incorporate the rotation into the Dirac algebra in a simple way. Since the public program is designed around this technique, it may be relatively easy to extend it to other lattice actions, such as highly improved actions.

V. CONCLUSIONS

In this paper we have set up a matching procedure, based on HQET, for heavy-heavy currents. It is valid for all $m_b a$ and $m_c a$, where m_b and m_c are the heavy quarks' masses and a is the lattice spacing. The procedure holds to all orders in perturbation theory and, therefore, potentially on a non-perturbative level also. It could be applied to lattice NRQCD, although here it is applied to Wilson fermions. With Wilson fermions it is possible to consider the limit of small $m_h a$. Then heavy-heavy HQET matching agrees with heavy-light HQET matching when the lighter quark satisfies $m_c a \ll 1$, and with Symanzik matching when both $m_h a \ll 1$. In this way, HQET matching is a natural and attractive extension into the regime $ma \not\ll 1$, which is needed for heavy-quark phenomenology on currently available computers.

The connection to heavy-light matching has an important implication for the charmed quark, whose mass is not necessarily large enough for the leading $1/m_c$ corrections to be accurate enough on their own. At the same time, however, the charmed mass is small enough that $m_c a \lesssim \frac{1}{3}$, on currently available lattices. In this regime the mismatches of short-distance coefficients of higher-dimension operators in HQET are influenced by the standard continuum limit (for the charmed quark), so they are easily kept down to the level of $\alpha_s m_c a$ and $(m_c a)^2$. Thus, more and more of the heavy-quark expansion is recovered, for masses where the higher-dimension terms may be significant.

Our one-loop results for the SW action are of immediate value for lattice calculations of form factors for the semi-leptonic decays $B \to D^{(*)} l\nu$. Indeed, our earlier one-loop results [16] (which omitted the "rotation" terms in the current) were used for $B \to D$ in Ref. [13], and our new results with rotation were used for $B \to D^*$ in Ref. [14]. In particular, we have obtained the BLM scale q^* for the renormalization factors, which reduces the uncertainty of one-loop calculations. Similarly, computing part of the normalization factor, namely $\sqrt{Z_{V_\parallel}^{cc} Z_{V_\parallel}^{bb}}$, non-perturbatively reduces the normalization uncertainty even further [13–15].

An outstanding problem at this time is the one-loop calculation of the coefficients $\bar{B}_{J_i}^{\rm lat}$ of the dimension-four terms in the HQET description. A calculation of these coefficients, and the subsequent adjustment of the parameters b_{J_i} in the lattice currents, would reduce the uncertainties in (future) calculations of $B \to D^{(*)}$ matrix elements. Because heavy-quark symmetry forbids several power corrections (see Refs. [1,14] for details), one must, however, also start to consider some of the dimension-five corrections to the currents.

ACKNOWLEDGMENTS

Dedicated to the memory of William E. Caswell, co-inventor of NRQED and NRQCD, who died September 11, 2001.

A.S.K. would like to thank Akira Ukawa and the Center for Computational Physics for hospitality while part of this work was being carried out, and the Aspen Center for Physics for a stimulating atmosphere while part of the paper was being written. S.H., A.S.K., and T.O. would also like to thank the Insititute for Nuclear Theory at the University of Washington for hospitality while this paper was being finished. S.H. and T.O. are supported by Grants-in-Aid of the Japanese Ministry of Education (Nos. 11740162 and 12640279, respectively).

Fermilab is operated by Universities Research Association Inc., under contract with the U.S. Department of Energy.

APPENDIX A: FEYNMAN RULES

The needed propagators and vertices for quark-gluon interactions are given already in Ref. [33]. Here we give the additional Feynman rules induced by the rotation term of the heavy quark. The additional rules are easy to derive by expressing the translation operator

$$T_{\pm\mu} = t_{\pm\mu/2} e^{\pm g_0 a A_\mu} t_{\pm\mu/2} \tag{A1}$$

and following the methods in Ref. [48].

There are six rules to give, with 0, 1, and 2 gluons emerging from the vertex; it is convenient to keep rules for gluons emitted from the incoming and outgoing rotations separate. Let the Dirac matrix of the current be Γ, and let

$$R(p) = 1 + i d_1 \sum_r \gamma_r \sin(p_r), \tag{A2}$$

$$R'(p') = 1 + i d_1' \sum_r \gamma_r \sin(p_r'). \tag{A3}$$

Then,

$$\text{0-gluon} = R'(p')\Gamma R(p), \tag{A4}$$

$$\text{1-gluon} = g_0 t^a d_1 \, R'(p')\Gamma\gamma_i \cos(p + \tfrac{1}{2}k)_i, \tag{A5}$$

$$\text{1-gluon}' = g_0 t^a d_1' \, \cos(p' - \tfrac{1}{2}k)_i \gamma_i \Gamma R(p), \tag{A6}$$

$$\text{2-gluon} = g_0^2 \tfrac{1}{2}\{t^a, t^b\}\delta_{ij} d_1 \, R'(p')\Gamma\gamma_i i \sin(p + \tfrac{1}{2}k + \tfrac{1}{2}\ell)_i \tag{A7}$$

$$\text{2-gluon}'' = g_0^2 \tfrac{1}{2}\{t^a, t^b\}\delta_{ij} d_1' \, i \sin(p' - \tfrac{1}{2}k - \tfrac{1}{2}\ell)_i \gamma_i \Gamma R(p) \tag{A8}$$

$$\text{2-gluon}' = g_0^2 t^b t^a \, d_1' d_1 \cos(p' - \tfrac{1}{2}\ell)_j \gamma_j \Gamma \gamma_i \cos(p + \tfrac{1}{2}k)_i \tag{A9}$$

where momentum p (p') is the quark momentum flowing into (out of) the vertex, and k and ℓ are gluon momentum flowing into vertex. In the two-gluon rules, there is *no* summation over i. As in Ref. [33], the matrices t^a are anti-Hermitian, *i.e.*, $U_\mu = \exp\left(g_0 t^a A_\mu^a\right)$, $\sum_{aj} t_{ij}^a t_{jk}^a = -C_F \delta_{ik}$, and $\mathrm{tr}\, t^a t^b = -\frac{1}{2}\delta^{ab}$.

APPENDIX B: DIRAC ALGEBRA

To compute the vertex function, there are eight diagrams to consider, depicted in Fig. 17: the usual vertex diagram (with the rotation inside), Fig. 17(a); two diagrams with the gluon connected to the incoming rotation, Fig. 17(b) and (c); a tadpole diagram connected to the incoming rotation [using rule (A7)], Fig. 17(d); a vertex diagram with a gluon connecting both rotations [using rule (A9)], Fig. 17(e); two diagrams with the gluon connected to the outgoing rotation, Fig. 17(f) and (g); and a tadpole diagram connected to the outgoing rotation, [using rule (A8)], Fig. 17(h). The two tadpole diagrams, Figs. 17(d) and (h), vanish for zero external three-momentum, because $\ell = -k$ and $p_i = 0$.

J	Γ	s_Γ
$V_\parallel$	γ_4	-1
$A_\perp$	$\gamma_j\gamma_5$	$+\frac{1}{3}$

TABLE I. The factor s_Γ, defined by $\frac{1}{3}\sum_r \gamma_r\Gamma\gamma_r = s_\Gamma\Gamma$.

For each non-vanishing diagram, Figs. 17(a–c, e–g), define the integral

$$I_\Gamma^{(\text{a–c, e–g})} = -g_0^2 C_F \int \frac{d^4k}{(2\pi)^4}\frac{1}{\hat{k}^2}\mathcal{I}_\Gamma^{(\text{a–c, e–g})}, \tag{B1}$$

where k is the momentum of the gluon in the loop, and $\hat{k}_\mu = 2\sin(\frac{1}{2}k_\mu)$. Let the incoming massive quark have couplings m_0, r_s, ζ, c_B, and c_E, and external momentum p. Similarly, let the outgoing massless quark have couplings $m_0' = 0$, r_s', ζ', c_B', and c_E', and external momentum p'. The internal quark lines carry momentum $p+k$ in and $p'+k$ out. The integrals I are obtained directly from the loop diagrams. Then

$$Z_J^{[1]} = \frac{1}{2}\left(Z_{2b\,\text{cont}}^{[1]} - Z_{2b\,\text{lat}}^{[1]} + Z_{2c\,\text{cont}}^{[1]} - Z_{2c\,\text{lat}}^{[1]}\right) + \sum_{\text{d}}\left(I_{\Gamma\,\text{cont}}^{\text{d}} - I_{\Gamma\,\text{lat}}^{\text{d}}\right), \tag{B2}$$

from Eq. (4.1). The relation between the current J and its Dirac matrix Γ is contained in Table I. The expression relating $Z_2^{[1]}{}_{\text{lat}}$ to lattice self-energy functions is in Ref. [33].

The most onerous task in evaluating the diagrams is the manipulation of the Dirac matrices. A convenient method is to treat each quark line separately, starting from the initial- or final-state spinor. Then the spinor, the propagator, and the vertices can be written out in 2×2 block diagonal form, with Pauli matrices appearing in the blocks. Once the Feynman rules are as complicated as in the present calculation, it is easier to manipulate 2×2 matrices of Pauli matrices than to manipulate Dirac matrices. A special advantage of this organization is that the rotation bracket in Eq. (A4) merely "rotates" the rest of the leg. We also obtain $Z_2^{[1]}{}_{\text{lat}}$ in this way, with much less effort than in Ref. [33].

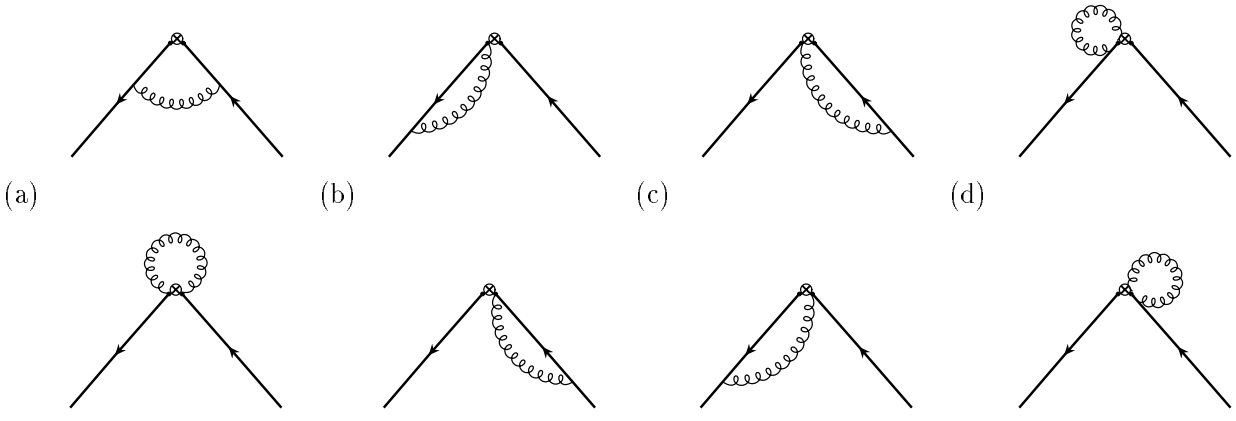

FIG. 17. Feynman diagrams for calculating the vertex function. The $\bullet$ on each side of the $\otimes$ indicates the rotation.

A further advantage is that the vertex corrections can be expressed compactly. The diagram with a gluon connecting the two rotations, Fig. 17(h), is

$$\mathcal{I}_\Gamma^{(\mathrm{e})} = s_\Gamma d_1' d_1 \sum_r \cos^2 \tfrac{1}{2} k_r. \tag{B3}$$

The diagrams with a gluon going from a leg to its own rotation, Figs. 17(b) and 17(f), are

$$\mathcal{I}_\Gamma^{(\mathrm{b})} = d_1 \frac{\zeta}{D} \left[(3 - \tfrac{1}{4}\hat{\boldsymbol{k}}^2) L + \tfrac{1}{2}\zeta \sum_r K_r S_r^2 \right], \tag{B4}$$

$$\mathcal{I}_\Gamma^{(\mathrm{f})} = d_1' \frac{\zeta'}{D'} \left[(3 - \tfrac{1}{4}\hat{\boldsymbol{k}}^2) L' + \tfrac{1}{2}\zeta' \sum_r K_r' S_r^2 \right], \tag{B5}$$

where $S_r = \sin k_r$, and the functions D, L, and K_r (and primed analogs) are given in Appendix C. The diagrams with a gluon going from a leg to the other rotation, Figs. 17(c) and 17(g), are

$$\mathcal{I}_\Gamma^{(\mathrm{c})} = s_\Gamma d_1 \frac{\zeta'}{D'} \left[(3 - \tfrac{1}{4}\hat{\boldsymbol{k}}^2) \mathcal{R}[L'] + \tfrac{1}{2} \mathcal{R}[\zeta'] \sum_r K_r' S_r^2 \right], \tag{B6}$$

$$\mathcal{I}_\Gamma^{(\mathrm{g})} = s_\Gamma d_1' \frac{\zeta}{D} \left[(3 - \tfrac{1}{4}\hat{\boldsymbol{k}}^2) \mathcal{R}[L] + \tfrac{1}{2} \mathcal{R}[\zeta] \sum_r K_r S_r^2 \right], \tag{B7}$$

where s_Γ is given in Table I.

The vertex diagram, Fig. 17(a), is complicated. We find $\mathcal{I}_\Gamma^{(\mathrm{a})} = N_\Gamma^{(\mathrm{a})}/DD'$, with numerator

$$N_\Gamma^{(\mathrm{a})} = \mathcal{R}[U_0'] \mathcal{R}[U_0] - s_\Gamma \mathcal{R}[L_0'] \mathcal{R}[L_0] \boldsymbol{S}^2 - \zeta\zeta' X_\Gamma. \tag{B8}$$

The part X_Γ comes from spatial gluon exchange:

$$X_\Gamma = -s_\Gamma (3 - \tfrac{1}{4}\hat{\boldsymbol{k}}^2) \mathcal{R}[L'] \mathcal{R}[L] \tag{B9}$$

$$+ s_\Gamma^2 (3 - \tfrac{1}{4}\hat{\boldsymbol{k}}^2) \mathcal{R}[V'] \mathcal{R}[V] \boldsymbol{S}^2 \tag{B10}$$

$$+ \tfrac{1}{2} \left(\mathcal{R}[V'] \mathcal{R}[U] - s_\Gamma \mathcal{R}[L'] \mathcal{R}[\zeta] \right) \sum_r K_r S_r^2 \tag{B11}$$

$$+ \tfrac{1}{2} \left(\mathcal{R}[U'] \mathcal{R}[V] - s_\Gamma \mathcal{R}[\zeta'] \mathcal{R}[L] \right) \sum_r K_r' S_r^2 \tag{B12}$$

$$+ \tfrac{1}{4} \left(\mathcal{R}[U'] \mathcal{R}[U] - s_\Gamma \boldsymbol{S}^2 \mathcal{R}[\zeta'] \mathcal{R}[\zeta] \right) \sum_r K_r' K_r \hat{k}_r^2 \tag{B13}$$

$$+ \tfrac{1}{8} (1 - s_\Gamma^2) \left(\hat{\boldsymbol{k}}^2 \boldsymbol{S}^2 - 3 \sum_r \hat{k}_r^2 S_r^2 \right) \mathcal{R}[V'] \mathcal{R}[V], \tag{B14}$$

where the last term is absent for V_4 (*i.e.*, when $s_\Gamma^2 = 1$). The rotation enters in the "rotated" functions

$$\mathcal{R}[U_0] = U_0 + d_1 \boldsymbol{S}^2 L_0, \tag{B15}$$

$$\mathcal{R}[L_0] = L_0 - d_1 U_0, \tag{B16}$$

$$\mathcal{R}[U] = U + d_1 \boldsymbol{S}^2 \zeta, \tag{B17}$$

$$\mathcal{R}[\zeta] = \zeta - d_1 U, \tag{B18}$$

$$\mathcal{R}[V] = V + d_1 L, \tag{B19}$$

$$\mathcal{R}[L] = L - d_1 \boldsymbol{S}^2 V, \tag{B20}$$

and similarly for primed functions. Although the vertex diagram is not easy to write down, the rotation modifies it in a fairly simple way, when using the 2×2 method described above.

We have verified that these expressions are correct by completely independent calculation with more common methods for the Dirac algebra.

APPENDIX C: USEFUL FUNCTIONS

In this appendix we list the functions appearing in Appendix B for the action and currents given in Sec. III. First, let

$$\mu = 1 + m_0 + \tfrac{1}{2} r_s \zeta \hat{\boldsymbol{k}}^2, \tag{C1}$$

$$\mu' = 1 + m'_0 + \tfrac{1}{2} r'_s \zeta' \hat{\boldsymbol{k}}^2. \tag{C2}$$

from now on a prime means to replace incoming coupling and momentum with corresponding outgoing coupling and momentum.

When the quark propagator is rationalized it has the denominator

$$D = 1 - 2\mu \cos(k_4 + i m_1^{[0]}) + \mu^2 + \zeta^2 \boldsymbol{S}^2, \tag{C3}$$

where $m_1^{[0]} = \log(1 + m_0)$.

In this calculation, the incoming and outgoing heavy quarks both have zero three-momentum, so both spinors consist only of upper components. This feature is different from the heavy-light case [2] and explains, at a low level, why the only dimension-three currents for heavy-heavy currents have $\Gamma = \gamma_4$ and $\gamma_j \gamma_5$ only.

To express the useful functions compactly, it is convenient to introduce first

$$U = \mu - e^{-m_1^{[0]} + i k_4}, \tag{C4}$$

$$\bar{U} = \mu - e^{+m_1^{[0]} - i k_4}, \tag{C5}$$

because these combinations appear in the other functions. Then

$$U_0 = U e^{+m_1^{[0]} - i k_4/2} - \tfrac{1}{2} \zeta^2 c_E \cos(\tfrac{1}{2} k_4) \boldsymbol{S}^2, \tag{C6}$$

$$L_0 = \zeta \left[e^{+m_1^{[0]} - i k_4/2} + \tfrac{1}{2} c_E \cos(\tfrac{1}{2} k_4) \bar{U} \right], \tag{C7}$$

$$V = \zeta \left[1 + \tfrac{i}{2} c_E \sin(k_4) \right] + \tfrac{1}{2} c_B U, \tag{C8}$$

$$L = -\bar{U} \left[1 + \tfrac{i}{2} c_E \sin(k_4) \right] + \tfrac{1}{2} c_B \zeta \boldsymbol{S}^2, \tag{C9}$$

$$K_r = r_s - c_B \cos^2(\tfrac{1}{2} k_r) = (r_s - c_B) + \tfrac{1}{4} c_B \hat{k}_r^2. \tag{C10}$$

Some related functions appear when the Dirac matrix connects upper and lower components, as in the case of heavy-light currents [2]. They will arise for heavy-heavy matching of the dimension-four currents, for which matrix elements with non-zero three-momentum must be calculated.

REFERENCES

* Present address: Yukawa Institute, Kyoto University.

[1] A. S. Kronfeld, Phys. Rev. D **62**, 014505 (2000) [hep-lat/0002008].

[2] J. Harada, S. Hashimoto, K.-I. Ishikawa, A. S. Kronfeld, T. Onogi, and N. Yamada, hep-lat/0112044.

[3] A. S. Kronfeld and P. B. Mackenzie, Annu. Rev. Nucl. Part. Sci. **43**, 793 (1993) [hep-ph/9303305]. For recent status, see S. Hashimoto, Nucl. Phys. B Proc. Suppl. **83**, 3 (2000) [hep-lat/9909136]; S. Aoki, in *Proceedings of the XIX International Symposium on Lepton and Photon Interactions at High Energy*, edited by J. A. Jaros and M. E. Peskin, eConfC **990809**, 657 (2000) [hep-ph/9912288]; S. Ryan, hep-lat/0111010.

[4] A. X. El-Khadra, A. S. Kronfeld, and P. B. Mackenzie, Phys. Rev. D **55**, 3933 (1997) [hep-lat/9604004].

[5] K. G. Wilson, in *New Phenomena in Subnuclear Physics*, edited by A. Zichichi (Plenum, New York, 1977).

[6] N. Isgur and M. B. Wise, Phys. Lett. B **232**, 113 (1989); **237**, 527 (1990).

[7] K. Symanzik, in *Recent Developments in Gauge Theories*, edited by G. 't Hooft *et al.* (Plenum, New York, 1980).

[8] K. Symanzik, in *Mathematical Problems in Theoretical Physics*, edited by R. Schrader *et al.* (Springer, New York, 1982); Nucl. Phys. B **226**, 187, 205 (1983).

[9] M. Lüscher, S. Sint, R. Sommer, and P. Weisz, Nucl. Phys. B **478**, 365 (1996) [hep-lat/9605038].

[10] K. Jansen *et al.*, Phys. Lett. B **372**, 275 (1996) [hep-lat/9512009]; M. Lüscher, S. Sint, R. Sommer, P. Weisz, and U. Wolff, Nucl. Phys. B **491**, 323 (1997) [hep-lat/9609035].

[11] B. Sheikholeslami and R. Wohlert, Nucl. Phys. B **259**, 572 (1985).

[12] A. S. Kronfeld, Nucl. Phys. B Proc. Suppl. **42**, 415 (1995) [hep-lat/9501002].

[13] S. Hashimoto *et al.*, Phys. Rev. D **61**, 014502 (2000) [hep-ph/9906376].

[14] S. Hashimoto *et al.*, hep-ph/0110253; J. N. Simone *et al.*, Nucl. Phys. B Proc. Suppl. **83**, 334 (2000) [hep-lat/9910026].

[15] A. X. El-Khadra, A. S. Kronfeld, P. B. Mackenzie, S. M. Ryan, and J. N. Simone, Phys. Rev. D **64**, 014502 (2001) [hep-ph/0101023].

[16] A. S. Kronfeld and S. Hashimoto, Nucl. Phys. B Proc. Suppl. **73**, 387 (1999) [hep-lat/9810042].

[17] S. J. Brodsky, G. P. Lepage, and P. B. Mackenzie, Phys. Rev. D **28**, 228 (1983).

[18] G. P. Lepage and P. B. Mackenzie, Phys. Rev. D **48**, 2250 (1993) [hep-lat/9209022].

[19] For the program, see http://theory.fnal.gov/people/kronfeld/LatHQ2QCD/ or the EPAPS Document accompanying this paper and Ref. [16]. With the latter method, go to the EPAPS home page http://www.aip.org/pubservs/epaps.html , or ftp.aip.org in the directory /epaps/. See the EPAPS home page for more information. (Of course, EPAPS is available only after publication.)

[20] E. Eichten, Nucl. Phys. B Proc. Suppl. **4**, 170 (1987).

[21] E. Eichten and B. Hill, Phys. Lett. B **234**, 511 (1990); **240**, 193 (1990).

[22] B. Grinstein, Nucl. Phys. B **339**, 253 (1990).

[23] H. Georgi, Phys. Lett. B **240**, 447 (1990).

[24] E. Eichten and B. Hill, Phys. Lett. B **243**, 427 (1990).

[25] W. E. Caswell and G. P. Lepage, Phys. Lett. B **167**, 437 (1986); G. T. Bodwin, E. Braaten and G. P. Lepage, Phys. Rev. D **46**, 1914 (1992) [hep-lat/9205006].
[26] G. P. Lepage and B. A. Thacker, Nucl. Phys. B Proc. Suppl. **4**, 199 (1987); B. A. Thacker and G. P. Lepage, Phys. Rev. D **43**, 196 (1991); G. P. Lepage, L. Magnea, C. Nakhleh, U. Magnea, and K. Hornbostel, *ibid.* **46**, 4052 (1992) [hep-lat/9205007].
[27] S. Hashimoto and H. Matsufuru, Phys. Rev. D **54**, 4578 (1996) [hep-lat/9511027].
[28] J. H. Sloan, Nucl. Phys. B Proc. Suppl. **63**, 365 (1998) [hep-lat/9710061].
[29] M. Luke and A. V. Manohar, Phys. Lett. B **286**, 348 (1992); M. Neubert, Phys. Lett. B **306**, 357 (1993); R. Sundrum, Phys. Rev. D **57**, 331 (1998).
[30] T. L. Trueman, Z. Phys. C **69**, 525 (1996) [hep-ph/9504315].
[31] C. T. H. Davies and B. A. Thacker, Phys. Rev. D **48**, 1329 (1993).
[32] P. Boyle and C. Davies, Phys. Rev. D **62**, 074507 (2000) [hep-lat/0003026].
[33] B. P. G. Mertens, A. S. Kronfeld, and A. X. El-Khadra, Phys. Rev. D **58**, 034505 (1998) [hep-lat/9712024].
[34] A. S. Kronfeld, Phys. Rev. D **58**, 051501 (1998) [hep-ph/9805215].
[35] Z. Sroczynski, hep-lat/0011059; Nucl. Phys. B Proc. Suppl. **83**, 971 (2000) [hep-lat/9910004].
[36] M. Neubert, Phys. Lett. B **341**, 367 (1995) [hep-ph/9409453].
[37] E. Gabrielli *et al.*, Nucl. Phys. B **362**, 475 (1991).
[38] G. Martinelli and Y. Zhang, Phys. Lett. B **123**, 433 (1983).
[39] G. P. Lepage, J. Comput. Phys. **27**, 192 (1978); Cornell University report CLNS-80/447 (unpublished, 1980).
[40] S. Kawabata, Comput. Phys. Commun. **88**, 309 (1995).
[41] K. Hornbostel, G. P. Lepage and C. Morningstar, Nucl. Phys. B Proc. Suppl. **94**, 579 (2001) [hep-lat/0011049].
[42] J. N. Simone, private communication. These values of $Z_{V_\parallel}^{\rm NP}$ were computed as part of Ref. [15].
[43] M. E. Luke, Phys. Lett. B **252**, 447 (1990).
[44] A. S. Kronfeld and B. P. Mertens, Nucl. Phys. B Proc. Suppl. **34**, 495 (1994) [hep-lat/9312042].
[45] Y. Kuramashi, Phys. Rev. D **58**, 034507 (1998) [hep-lat/9705036].
[46] K.-I. Ishikawa, S. Aoki, S. Hashimoto, H. Matsufuru, T. Onogi, and N. Yamada, Nucl. Phys. B Proc. Suppl. **63**, 344 (1998) [hep-lat/9711005]; K.-I. Ishikawa, T. Onogi, and N. Yamada, Nucl. Phys. B Proc. Suppl. **83**, 301 (2000) [hep-lat/9909159].
[47] J. Harada, A. S. Kronfeld, H. Matsufuru, N. Nakajima and T. Onogi, Phys. Rev. D **64**, 074501 (2001) [hep-lat/0103026].
[48] A. S. Kronfeld and D. M. Photiadis, Phys. Rev. D **31**, 2939 (1985).